J. Fluid Mech. (2012), *vol.* 710, *pp.* 379–418.
doi:10.1017/jfm.2012.370

On the steady-state fully resonant progressive waves in water of finite depth

Dali Xu[2], Zhiliang Lin[2], Shijun Liao[1,2]† and Michael Stiassnie[3]

[1] State Key Laboratory of Ocean Engineering, Shanghai Jiao Tong University, Shanghai 200240, China

[2] School of Naval Architecture, Ocean and Civil Engineering, Shanghai Jiao Tong University, Shanghai 200240, China

[3] Faculty of Civil and Environmental Engineering, Technion IIT, Haifa 32000, Israel

(Received 14 January 2012; revised 30 June 2012; accepted 17 July 2012; first published online 7 September 2012)

The steady-state fully resonant wave system, consisting of two progressive primary waves in finite water depth and all components due to nonlinear interaction, is investigated in detail by means of analytically solving the fully nonlinear wave equations as a nonlinear boundary-value problem. It is found that multiple steady-state fully resonant waves exist in some cases which have no exchange of wave energy at all, so that the energy spectrum is time-independent. Further, the steady-state resonant wave component may contain only a small proportion of the wave energy. However, even in these cases, there usually exist time-dependent periodic exchanges of wave energy around the time-independent energy spectrum corresponding to such a steady-state fully resonant wave, since it is hard to be exactly in such a balanced state in practice. This view serves to deepen and enrich our understanding of the resonance of gravity waves.

Key words: surface gravity waves

1. Introduction

In physics, resonance is the tendency of a system to oscillate at a greater amplitude at some frequencies, i.e. the system's resonance frequencies, than at others. At these frequencies, even small periodic driving forces can often produce large-amplitude oscillations, because the system stores vibrational energy.

The so-called gravity wave resonance has been a hot topic in fluid mechanics since the last century. In his pioneering work, Phillips (1960, 1981) found the resonance criterion of a quartet of progressive waves in deep water,

$$\boldsymbol{k}_1 \pm \boldsymbol{k}_2 \pm \boldsymbol{k}_3 \pm \boldsymbol{k}_4 = 0, \quad \omega_1 \pm \omega_2 \pm \omega_3 \pm \omega_4 = 0, \tag{1.1}$$

where $\boldsymbol{k}_i$ denotes the wavenumber, $\omega_i = \sqrt{g k_i}$ with $k_i = |\boldsymbol{k}_i|$ is the angular frequency, g is the acceleration due to gravity, respectively. In particular, when two of the four waves have the same wavenumber, say, $\boldsymbol{k}_1 = \boldsymbol{k}_4$, so that

$$\boldsymbol{k}_3 = 2\boldsymbol{k}_1 - \boldsymbol{k}_2, \quad \omega_3 = 2\omega_1 - \omega_2, \tag{1.2}$$

† Email address for correspondence: sjliao@sjtu.edu.cn

the corresponding resonance criterion leads to

$$(2\omega_1 - \omega_2)^2 = g|2\boldsymbol{k}_1 - \boldsymbol{k}_2|, \tag{1.3}$$

which comes from the dispersion relation $\omega_3^2 = gk_3$ given by the linear wave theory. In this special case, Phillips (1960) found that the amplitude of the resonant wave component, if it is zero initially, grows linearly with time. This conclusion for small times was verified later by Longuet-Higgins (1962) using perturbation methods. Meanwhile, in order to find the physical mechanism of wave resonance, Benney (1962) established the evolution equations of wave mode amplitudes, and demonstrated the well-known time-dependent periodic exchange of wave energy governed by Jacobian elliptic functions, when Phillips' resonance criterion is fully or nearly satisfied. Following Benney's excellent work, Bretherton (1964) solved the evolution equations of the oscillation amplitudes over a characteristic time.

To check the theoretical results some experiments were done. Longuet-Higgins & Smith (1966) and McGoldrick *et al.* (1966) experimentally studied the interaction of two mutually orthogonal primary wave trains generated in a wave tank, and identified the resonant wave whose amplitude grows with the interaction distance. It was found that the resonant wave does not appear when Phillips' resonant condition is not satisfied. This experiment demonstrated wave resonance for the first time.

The above-mentioned studies were on resonant waves in deep water. In the shallow water case, Phillips (1960) pointed out that any pair of parallel gravity waves would interact resonantly with each other, because they have no dispersive property. Recently, based on the quadratic Boussinesq equations, Onorato *et al.* (2009) studied the energy transfer of shallow water waves, and found that the four-wave resonant interactions are included naturally. Katsardi & Swan (2011) studied numerically the evolution of waves propagating unidirectionally in intermediate and shallow water, and found that the third-order resonant term is the dominant influence as the water depth reduces.

Following the pioneering work of Phillips (1960), most researchers have focused on the evolution of resonant waves whose amplitude is zero at $t = 0$. Obviously, Phillips' result for a linearly growing resonant wave amplitude is valid only for short times, otherwise the resonant wave would contain all the wave energy, which is, however, physically impossible. Physically speaking, if the viscosity of the fluid is neglected, the wave system should be in some kind of stable balanced state if the time is sufficiently long. As discovered by Benney (1962), one such balanced state corresponds to the time-dependent periodic exchange of wave energy between different wave components. Does there exist some form of balanced state for which there is no exchange of wave energy at all when Phillips' resonance criterion is fully satisfied?

Liao (2011) investigated this kind of steady state for the nonlinear interaction of two trains of propagating waves in deep water. Here, the steady state means that there is no exchange at all of wave energy between different wave components, that is, all amplitudes of wave components are independent of time. By means of the so-called homotopy analysis method (HAM) developed by Liao (1992, 1999, 2003, 2010, 2012), a powerful analytic method for highly nonlinear problems, the exact nonlinear wave equations were solved and the convergent series solutions were obtained in both resonant and non-resonant cases. Liao (2011) found, for the first time, that this kind of steady-state wave system has three different solutions when Phillips' resonance criterion is satisfied! In particular, it is found that, although the amplitude of the resonant wave component is of the same order as that of the two primary waves, it is not always the largest one. In some cases, the amplitude of the resonant wave component is much smaller than the primary ones, i.e. the resonant wave components can contain only a small proportion of the total wave energy.

In this article, in order to confirm the above conclusions of Liao (2011) in general cases, we further investigate this kind of steady-state system for the nonlinear interaction of two trains of waves propagating in water of finite depth, when Phillips' resonance condition is exactly satisfied. This steady-state wave system, if it does indeed exist, has steady wavenumber, frequency and amplitude for each wave component, which are independent of time. Using the HAM in a similar way, we obtain six different steady-state resonant waves, three more than those given by Liao (2011). Further, it is found once again that the amplitude of the resonant component is not always dominant: it can be much smaller than that of the primary ones in some cases. This confirms that Liao's conclusions (2011) concerning steady-state resonant waves in deep water also hold for steady-state resonant waves in finite water depth and thus have general application. Furthermore, the effect of the water depth on steady-state resonant waves is investigated for the first time. All of this will help to deepen and enrich our understanding of the resonance for gravity waves.

This paper is organized as follows. The mathematical description of the physical problem is given in § 2. The basic idea of the solution procedure in the HAM context is described in § 3. The multiple solutions of the steady-state resonant waves for a particular case are given in § 4. The multiple solutions of steady-state resonant waves for some other cases are presented in § 5. Concluding remarks and discussions follow in § 6. The detailed mathematical formulas related to the HAM are given in appendix A. Our main conclusions are confirmed by means of Zakharov's equation, as described briefly in appendix B.

2. The mathematical description

2.1. *The original initial/boundary-value problem*

Let us consider the nonlinear interactions of two trains of progressive gravity waves with small amplitudes, propagating in water of finite depth d. We assume that the fluid is inviscid and incompressible, the flow is irrotational, and the surface tension is neglected. The coordinate system (x, y, z) is set on the free surface, with z-axis positive vertically from the free surface. The governing equation of the velocity potential $\phi(x, y, z, t)$ is given by

$$\nabla^2\phi = 0, \quad -d < z < \eta(x, y, t), \tag{2.1}$$

subject to the two boundary conditions on the unknown free surface $z = \eta(x, y, t)$,

$$\frac{\partial^2\phi}{\partial t^2} + g\frac{\partial\phi}{\partial z} + \frac{\partial\,|\nabla\phi|^2}{\partial t} + \nabla\phi\cdot\nabla\left(\frac{1}{2}\,|\nabla\phi|^2\right) = 0, \tag{2.2}$$

$$g\eta + \frac{\partial\phi}{\partial t} + \frac{1}{2}\,|\nabla\phi|^2 = 0, \tag{2.3}$$

and the bottom boundary condition

$$\frac{\partial\phi}{\partial z} = 0 \quad \text{at } z = -d, \tag{2.4}$$

where

$$\nabla = \boldsymbol{i}\frac{\partial}{\partial x} + \boldsymbol{j}\frac{\partial}{\partial y} + \boldsymbol{k}\frac{\partial}{\partial z} \tag{2.5}$$

is a linear operator, with $\boldsymbol{i}, \boldsymbol{j}, \boldsymbol{k}$ denoting unit vectors in the x, y, z directions, respectively. Here all variables are dimensional.

2.2. *Solution formulas*

Although the governing equation (2.1) and the bottom boundary condition (2.4) are linear, the two nonlinear boundary conditions (2.2) and (2.3) are satisfied on the unknown free surface $\eta(x, y, t)$. Such nonlinear partial differential equations (PDEs) are difficult to solve in general, often with rather complicated solutions. However, when the so-called steady-state wave system with time-independent wavenumber, frequency and amplitude for each component does indeed exist, the corresponding velocity potential $\phi(x, y, z, t)$ and the wave elevation $\eta(x, y, t)$ have rather simple expressions, as shown below. Our goal is to discover such steady-state resonant waves when they do indeed exist.

By means of perturbation methods, Benney (1962) and Bretherton (1964) assumed that, when there are l primary waves, the wave elevation has the form

$$\eta = \sum_l \{A_l(\tau)\exp[\mathrm{i}(\boldsymbol{k}_l \cdot \boldsymbol{r} - \omega_l t)] + A_{-l}(\tau)\exp[-\mathrm{i}(\boldsymbol{k}_l \cdot \boldsymbol{r} - \omega_l t)]\}, \quad l = 1, 2, \ldots, \tag{2.6}$$

where $\mathrm{i} = \sqrt{-1}$, $\tau = \varepsilon t$, $A_{-l}(\tau)$ is the complex conjugate of $A_l(\tau)$, ε is a small parameter that makes $A_l(\tau)$ a slowly varying function, $\boldsymbol{k}_l$ is the wavenumber of the lth primary wave and $\omega_l^2 = g|\boldsymbol{k}_l|$ corresponds to the classical linear theory, and $\boldsymbol{r} = x\boldsymbol{i} + y\boldsymbol{j}$ is a spatial vector for (x, y), respectively. Similar expressions can also be found in the monograph by Craik (1988). Benney (1962) and Bretherton (1964) gave the evolution equations of $A_l(\tau)$ and found that $A_l(\tau)$ can be expressed in terms of elliptic functions.

Assume that steady-state resonant waves exist, so that the corresponding wave elevation can be expressed by

$$\eta(x, y, t) = \sum_{l=1}^{+\infty} \overline{A}_l \cos(\boldsymbol{k}_l \cdot \boldsymbol{r} - \sigma_l t), \tag{2.7}$$

where $\overline{A}_l$ is a constant and σ_l is the actual frequency. Note that, due to weakly nonlinear effects, the actual frequencies of waves, σ_1 and σ_2, are often slightly different from the linear dispersion relation $\omega_l = \sqrt{gk_l \tanh(k_l d)}$ and also depend on the wave amplitudes. The above formula provides the solution for the wave elevation.

Note that the existence of steady-state resonant waves is merely assumed here. Our strategy is first to make this assumption and then to prove that the corresponding steady-state resonant waves do indeed exist in some cases, if they satisfy the fully nonlinear wave equation (2.1)–(2.4). If no such steady-state solutions can be found, it indicates that the assumption is wrong, that is, no steady-state resonant waves can exist. In this way, we can investigate the existence of steady-state resonant waves in detail.

For simplicity, let us consider a steady-state resonant wave system consisting of two primary progressive waves with wavenumbers $\boldsymbol{k}_1$ and $\boldsymbol{k}_2$. According to the elevation expression (2.7), we define the two variables

$$\xi_1 = \boldsymbol{k}_1 \cdot \boldsymbol{r} - \sigma_1 t, \quad \xi_2 = \boldsymbol{k}_2 \cdot \boldsymbol{r} - \sigma_2 t, \tag{2.8}$$

related to the two primary waves, with the definitions

$$\boldsymbol{r} = x\boldsymbol{i} + y\boldsymbol{j}, \tag{2.9}$$

$$\boldsymbol{k}_1 = k_1(\cos\alpha_1\boldsymbol{i} + \sin\alpha_1\boldsymbol{j}), \tag{2.10}$$

$$\boldsymbol{k}_2 = k_2(\cos\alpha_2\boldsymbol{i} + \sin\alpha_2\boldsymbol{j}), \tag{2.11}$$

where $k_l = |\boldsymbol{k}_l|$ and α_l $(l = 1, 2)$ is the angle between the x-axis and the wavenumber vector $\boldsymbol{k}_l$, σ_l is the wave angular frequency of the lth primary wave, respectively. Using the new variables ξ_1, ξ_2 and the solution expression (2.7), the wave elevation $\eta(x, y, t)$ of a steady-state resonant wave system is expressed by

$$\eta(\xi_1, \xi_2) = \sum_{m=0}^{+\infty}\sum_{n=-\infty}^{+\infty} a_{m,n}\cos(m\xi_1 + n\xi_2), \tag{2.12}$$

where $a_{m,n}$ is a constant to be determined later. Note that the time t does not appear in the above expression. Accordingly, the velocity potential ϕ is dependent only upon ξ_1, ξ_2 and z. Then, using the above definitions, the governing equation (2.1) becomes

$$k_1^2\frac{\partial^2\phi}{\partial\xi_1^2} + 2\boldsymbol{k}_1\cdot\boldsymbol{k}_2\frac{\partial^2\phi}{\partial\xi_1\partial\xi_2} + k_2^2\frac{\partial^2\phi}{\partial\xi_2^2} + \frac{\partial^2\phi}{\partial z^2} = 0, \quad -d < z < \eta(\xi_1, \xi_2), \tag{2.13}$$

subject to the boundary conditions on the unknown free surface $z = \eta(\xi_1, \xi_2)$,

$$\sigma_1^2\frac{\partial^2\phi}{\partial\xi_1^2} + 2\sigma_1\sigma_2\frac{\partial^2\phi}{\partial\xi_1\partial\xi_2} + \sigma_2^2\frac{\partial^2\phi}{\partial\xi_2^2} + g\frac{\partial\phi}{\partial z} - 2\left(\sigma_1\frac{\partial f}{\partial\xi_1} + \sigma_2\frac{\partial f}{\partial\xi_2}\right) + \hat{\boldsymbol{\nabla}}\phi\cdot\hat{\boldsymbol{\nabla}}f = 0, \tag{2.14}$$

$$\eta = \frac{1}{g}\left(\sigma_1\frac{\partial\phi}{\partial\xi_1} + \sigma_2\frac{\partial\phi}{\partial\xi_2} - f\right), \tag{2.15}$$

and the bottom condition

$$\frac{\partial\phi}{\partial z} = 0 \quad \text{at } z = -d, \tag{2.16}$$

where

$$\hat{\boldsymbol{\nabla}} = \boldsymbol{k}_1\frac{\partial}{\partial\xi_1} + \boldsymbol{k}_2\frac{\partial}{\partial\xi_2} + \boldsymbol{k}\frac{\partial}{\partial z}, \tag{2.17}$$

and

$$f = \frac{1}{2}\left[k_1^2\left(\frac{\partial\phi}{\partial\xi_1}\right)^2 + 2\boldsymbol{k}_1\cdot\boldsymbol{k}_2\frac{\partial\phi}{\partial\xi_1}\frac{\partial\phi}{\partial\xi_2} + k_2^2\left(\frac{\partial\phi}{\partial\xi_2}\right)^2 + \left(\frac{\partial\phi}{\partial z}\right)^2\right]. \tag{2.18}$$

Note that the time t disappears in all the above equations. In this way, the original initial/boundary-value problem (2.1)–(2.4) becomes a nonlinear boundary-value one, mainly because we are only interested in the steady-state resonant waves but completely neglect the corresponding initial conditions for them.

According to the linear governing equation (2.13) and the bottom boundary condition (2.16), the velocity potential $\phi(\xi_1, \xi_2, z)$ should be in the form

$$\phi(\xi_1, \xi_2, z) = \sum_{m=0}^{+\infty}\sum_{n=-\infty}^{+\infty} b_{m,n}\Psi_{m,n}(\xi_1, \xi_2, z) \tag{2.19}$$

with the definition

$$\Psi_{m,n} = \sin(m\xi_1 + n\xi_2)\frac{\cosh[|m\boldsymbol{k}_1 + n\boldsymbol{k}_2|(z+d)]}{\cosh[|m\boldsymbol{k}_1 + n\boldsymbol{k}_2|d]}, \tag{2.20}$$

where $b_{m,n}$ is a constant to be determined. Note that (2.19) automatically satisfies the linear governing equation (2.13) and the bottom boundary condition (2.16). From a mathematical viewpoint, our aim is to find the velocity potential $\phi(\xi_1, \xi_2, z)$ and the elevation $\eta(\xi_1, \xi_2)$ in the form of (2.12) and (2.19), respectively, which satisfy the two nonlinear boundary conditions (2.14) and (2.15) on the free surface $z = \eta(\xi_1, \xi_2)$.

3. Analytic approach based on the homotopy analysis method

In this section, the nonlinear boundary-value problem governed by the PDEs (2.13)–(2.16) is solved by means of the homotopy analysis method.

Traditionally, perturbation methods have been widely applied to solve nonlinear problems related to gravity waves. It is well known that perturbation methods are strongly dependent upon small physical parameters, i.e. the so-called perturbation quantities. To overcome the restrictions of perturbation methods and some traditional non-perturbation techniques, Liao (1992, 1999, 2003, 2010, 2012) developed an analytic technique for highly nonlinear problems, namely the homotopy analysis method (HAM). Unlike perturbation techniques, the HAM is entirely independent of small physical parameters. Further, being based on the homotopy concept in topology, the HAM gives us great freedom in the choice of the initial guess, the equation type of linear subproblems and the basis functions of solution. In particular, unlike all other analytic techniques, the HAM provides a simple way to guarantee the convergence of approximations and is thus valid for highly nonlinear problems in general. For example, unlike asymptotic/perturbation formulas, which are often valid only a couple of days or weeks prior to expiry, the optimal exercise boundary of an American put option given by Liao (2012) (see chapter 13) using the HAM may be valid for a couple of dozen years or even half a century. For details on the HAM, refer to the two books by Liao (2003, 2012).

3.1. *Continuous variation*

Let $\phi_0(\xi_1, \xi_2, z)$, $\eta_0(\xi_1, \xi_2)$ denote the initial guesses of the steady-state velocity potential $\phi(\xi_1, \xi_2, z)$ and wave elevation $\eta(\xi_1, \xi_2)$, respectively. For simplicity, we choose $\eta_0(\xi_1, \xi_2) = 0$. Let $q \in [0, 1]$ denote an embedding parameter and let $c_0 \neq 0$ be the so-called convergence-control parameter. Here, both q and c_0 are auxiliary parameters without physical meaning. Instead of solving the nonlinear PDEs (2.13)–(2.16) directly, we first construct a family (with respect to q) of PDEs about two continuous variations $\breve{\phi}(\xi_1, \xi_2, z; q)$ and $\breve{\eta}(\xi_1, \xi_2; q)$, governed by the so-called zeroth-order deformation equations,

$$\hat{\nabla}^2\breve{\phi}(\xi_1, \xi_2, z; q) = 0, \quad -d < z < \breve{\eta}(\xi_1, \xi_2; q), \tag{3.1}$$

subject to the two boundary conditions on the unknown free surface $z = \breve{\eta}(\xi_1, \xi_2; q)$,

$$(1-q)\mathscr{L}[\breve{\phi}(\xi_1, \xi_2, z; q) - \phi_0(\xi_1, \xi_2, z)] = qc_0\mathscr{N}_1[\breve{\phi}(\xi_1, \xi_2, z; q)], \tag{3.2}$$

$$(1-q)\breve{\eta}(\xi_1, \xi_2; q) = qc_0\mathscr{N}_2[\breve{\eta}(\xi_1, \xi_2; q), \breve{\phi}(\xi_1, \xi_2, z; q)], \tag{3.3}$$

and the bottom condition

$$\frac{\partial\breve{\phi}(\xi_1, \xi_2, z; q)}{\partial z} = 0 \quad \text{at } z = -d, \tag{3.4}$$

where $\mathscr{L}$ is an auxiliary linear operator with the property $\mathscr{L}(0)=0$, $\mathscr{N}_1$ and $\mathscr{N}_2$ are nonlinear differential operators defined by

$$\mathscr{N}_1[\breve{\phi}] = \sigma_1^2\frac{\partial^2\breve{\phi}}{\partial\xi_1^2} + 2\sigma_1\sigma_2\frac{\partial^2\breve{\phi}}{\partial\xi_1\partial\xi_2} + \sigma_2^2\frac{\partial^2\breve{\phi}}{\partial\xi_2^2} + g\frac{\partial\breve{\phi}}{\partial z} - 2\left(\sigma_1\frac{\partial\breve{f}}{\partial\xi_1} + \sigma_2\frac{\partial\breve{f}}{\partial\xi_2}\right) + \hat{\nabla}\breve{\phi}\cdot\hat{\nabla}\breve{f}, \tag{3.5}$$

$$\mathscr{N}_2[\breve{\eta},\breve{\phi}] = \breve{\eta}(\xi_1,\xi_2;q) - \frac{1}{g}\left[\sigma_1\frac{\partial\breve{\phi}(\xi_1,\xi_2,z;q)}{\partial\xi_1} + \sigma_2\frac{\partial\breve{\phi}(\xi_1,\xi_2,z;q)}{\partial\xi_2} - \breve{f}\right], \tag{3.6}$$

with the definition

$$\breve{f} = \tfrac{1}{2}\hat{\nabla}\breve{\phi}\cdot\hat{\nabla}\breve{\phi}. \tag{3.7}$$

Note that the definitions of $\mathscr{N}_1$ and $\mathscr{N}_2$ are based on the two boundary conditions (2.14) and (2.15), respectively.

When $q=0$, the zeroth-order deformation equations (3.1)–(3.4) have the solution

$$\breve{\phi}(\xi_1,\xi_2,z;0) = \phi_0(\xi_1,\xi_2,z), \tag{3.8}$$
$$\breve{\eta}(\xi_1,\xi_2;0) = \eta_0(\xi_1,\xi_2) = 0. \tag{3.9}$$

When $q=1$, the zeroth-order deformation equations (3.1)–(3.4) are equivalent to the original PDEs (2.13)–(2.16), so we have the solution

$$\breve{\phi}(\xi_1,\xi_2,z;1) = \phi(\xi_1,\xi_2,z), \tag{3.10}$$
$$\breve{\eta}(\xi_1,\xi_2;1) = \eta(\xi_1,\xi_2). \tag{3.11}$$

Thus, as the embedding parameter $q\in[0,1]$ increases from 0 to 1, $\breve{\phi}(\xi_1,\xi_2,z;q)$ and $\breve{\eta}(\xi_1,\xi_2;q)$ vary continuously from their initial guess solutions $\phi_0(\xi_{21},\xi_2,z)$ and $\eta_0(\xi_1,\xi_2)=0$ to the exact velocity potential $\phi(\xi_1,\xi_2,z)$ and the wave elevation $\eta(\xi_1,\xi_2)$, respectively. Thus, the zeroth-order deformation equations (3.1)–(3.4) indeed construct two continuous variations $\breve{\phi}(\xi_1,\xi_2,z;q)$ and $\breve{\eta}(\xi_1,\xi_2;q)$. Such continuous variations (or deformations) are called homotopies in topology, expressed by

$$\breve{\phi}(\xi_1,\xi_2,z;q) : \phi_0(\xi_1,\xi_2,z) \sim \phi(\xi_1,\xi_2,z), \tag{3.12}$$
$$\breve{\eta}(\xi_1,\xi_2;q) : \eta_0(\xi_1,\xi_2) \sim \eta(\xi_1,\xi_2). \tag{3.13}$$

It should be emphasized that the above two continuous deformations are also dependent upon the convergence-control parameter c_0, which has no physical meaning but provides a convenient way to guarantee the convergence of approximations, as shown later. In fact, it is the so-called convergence-control parameter c_0 that differentiates the HAM from all other analytic techniques, as pointed out by Liao (2012).

The Maclaurin series of $\breve{\phi}(\xi_1,\xi_2,z;q)$ and $\breve{\eta}(\xi_1,\xi_2;q)$, with respect to the embedding parameter $q\in[0,1]$, reads

$$\breve{\phi}(\xi_1,\xi_2,z;q) = \sum_{n=0}^{+\infty}\phi_n(\xi_1,\xi_2,z)q^n, \tag{3.14}$$

$$\breve{\eta}(\xi_1,\xi_2;q) = \sum_{n=0}^{+\infty}\eta_n(\xi_1,\xi_2)q^n, \tag{3.15}$$

where

$$\phi_n(\xi_1, \xi_2, z) = \frac{1}{n!} \frac{\partial^n \check{\phi}(\xi_1, \xi_2, z; q)}{\partial q^n}\bigg|_{q=0}, \tag{3.16}$$

$$\eta_n(\xi_1, \xi_2) = \frac{1}{n!} \frac{\partial^n \check{\eta}(\xi_1, \xi_2; q)}{\partial q^n}\bigg|_{q=0}. \tag{3.17}$$

Using (3.10) and (3.11) and assuming that the convergence-control parameter c_0 is properly chosen so that the Maclaurin series (3.14) and (3.15) are convergent at $q=1$, we have the so-called homotopy-series solution

$$\phi(\xi_1, \xi_2, z) = \phi_0(\xi_1, \xi_2, z) + \sum_{n=1}^{+\infty} \phi_n(\xi_1, \xi_2, z), \tag{3.18}$$

$$\eta(\xi_1, \xi_2) = \sum_{n=1}^{+\infty} \eta_n(\xi_1, \xi_2). \tag{3.19}$$

As shown later in § 3.2, the unknown term $\phi_n(\xi_1, \xi_2, z)$ is governed by a linear PDE, and it is straightforward to obtain $\eta_n(\xi_1, \xi_2)$ as long as $\phi_{n-1}(\xi_1, \xi_2, z)$ is known. In this way, the original nonlinear PDEs (2.13)–(2.16) are transformed into an infinite number of linear PDEs. However, unlike perturbation techniques, such transformation in the context of the HAM does not need any small physical parameters. Further, being based on the concept of homotopy in topology, it gives us great freedom in the choice of auxiliary linear operator $\mathscr{L}$, the convergence-control parameter c_0 and the initial guess $\phi_0(\xi_1, \xi_2, z)$, which greatly simplifies resolution of the nonlinear PDEs, as shown below.

Since the HAM provides freedom in the choice of auxiliary linear operator, and considering the linear part of (2.14), we choose

$$\mathscr{L}\phi = \left(\omega_1^2 \frac{\partial^2 \phi}{\partial \xi_1^2} + 2\omega_1\omega_2 \frac{\partial^2 \phi}{\partial \xi_1 \partial \xi_2} + \omega_2^2 \frac{\partial^2 \phi}{\partial \xi_2^2} + g\frac{\partial \phi}{\partial z} \right), \tag{3.20}$$

where

$$\omega_1 = \sqrt{g k_1 \tanh(k_1 d)}, \quad \omega_2 = \sqrt{g k_2 \tanh(k_2 d)} \tag{3.21}$$

are given by linear wave theory. The above auxiliary linear operator has the property

$$\mathscr{L}\Psi_{m,n} = \lambda_{m,n}\Psi_{m,n}, \tag{3.22}$$

where

$$\lambda_{m,n} = -(m\omega_1 + n\omega_2)^2 + g|m\boldsymbol{k}_1 + n\boldsymbol{k}_2| \tanh(|m\boldsymbol{k}_1 + n\boldsymbol{k}_2|d) \tag{3.23}$$

can be regarded as an eigenvalue of $\mathscr{L}$. Thus, $\Psi_{m,n}$ defined by (2.20) can also be regarded as a corresponding eigenfunction of the auxiliary linear operator $\mathscr{L}$.

3.2. *High-order deformation equation*

Differentiating the zeroth-order deformation equations (3.1)–(3.4) m times with respect to q, then dividing them by $m!$ and setting $q=0$, we have the mth-order deformation equation

$$\hat{\nabla}^2\phi_m = 0, \quad -d < z < 0, \tag{3.24}$$

subject to the two boundary conditions at $z=0$,

$$\bar{\mathscr{L}}[\phi_m] = c_0\Delta^{\phi}_{m-1}(\xi_1,\xi_2) - \bar{S}_m(\xi_1,\xi_2) + \chi_m S_{m-1}(\xi_1,\xi_2), \tag{3.25}$$

$$\eta_m = c_0\Delta^{\eta}_{m-1}(\xi_1,\xi_2) + \chi_m\eta_{m-1}, \tag{3.26}$$

and the bottom condition

$$\frac{\partial\phi_m}{\partial z} = 0 \quad z=-d, \tag{3.27}$$

where

$$\chi_m = \begin{cases} 0 & \text{when } m \leqslant 1, \\ 1 & \text{when } m > 1. \end{cases} \tag{3.28}$$

The detailed expressions of $\Delta^{\phi}_{m-1}(\xi_1,\xi_2)$, $\bar{S}_m(\xi_1,\xi_2)$, $S_{m-1}(\xi_1,\xi_2)$ and $\Delta^{\eta}_{m-1}(\xi_1,\xi_2)$ are given in appendix A, and the linear operator $\bar{\mathscr{L}}$ is defined by

$$\bar{\mathscr{L}}[\phi_m] = \left(\omega_1^2\frac{\partial^2\phi_m}{\partial\xi_1^2} + 2\omega_1\omega_2\frac{\partial^2\phi_m}{\partial\xi_1\partial\xi_2} + \omega_2^2\frac{\partial^2\phi_m}{\partial\xi_2^2} + g\frac{\partial\phi_m}{\partial z}\right)\bigg|_{z=0}, \tag{3.29}$$

with the property

$$\bar{\mathscr{L}}^{-1}[\sin(m\xi_1+n\xi_2)] = \frac{\Psi_{m,n}}{\lambda_{m,n}}, \quad \lambda_{m,n}\neq 0. \tag{3.30}$$

For details, refer to Liao (2011, 2012). Note that the right-hand sides of (3.25) and (3.26) are only related to approximations at lower orders and are thus regarded as known. So, it is straightforward to obtain η_m by means of (3.26). Further, $\Psi_{m,n}$ defined by (2.20) automatically satisfies the Laplace equation (3.24) and the boundary condition (3.27) at bottom. So,

$$\phi_m^* = \bar{\mathscr{L}}^{-1}\left[c_0\Delta^{\phi}_{m-1}(\xi_1,\xi_2) - \bar{S}_m(\xi_1,\xi_2) + \chi_m S_{m-1}(\xi_1,\xi_2)\right] \tag{3.31}$$

gives a special solution of ϕ_m. Thus, by means of the inverse operator (3.30) and a computer algebra system such as Mathematica, it is easy to solve the high-order deformation equation (3.24) with the linear boundary conditions (3.25)–(3.27).

3.3. *Initial guess of potential function*

As mentioned by Chen (1990), Phillips' resonance criterion of four small-amplitude waves in water of finite depth, when two of them are equal, reads

$$(2\omega_1-\omega_2)^2 = g|2\boldsymbol{k}_1-\boldsymbol{k}_2|\tanh(|2\boldsymbol{k}_1-\boldsymbol{k}_2|d), \tag{3.32}$$

where ω_1 and ω_2 are defined by (3.21). It is interesting that, according to (3.23), we have $\lambda_{2,-1}=0$ when the above resonance criterion (3.32) is satisfied. Further, according to (3.23), we always have $\lambda_{1,0}\equiv 0$ and $\lambda_{0,1}\equiv 0$, no matter whether the resonance criterion (3.32) is satisfied. In other words, there are three zero eigenvalues $\lambda_{1,0}$, $\lambda_{0,1}$ and $\lambda_{2,-1}$ when Phillips' resonance criterion (3.32) is satisfied. Thus, from a mathematical viewpoint, the common solution of ϕ_m reads

$$\phi_m = \phi_m^* + A_m\Psi_{1,0} + B_m\Psi_{0,1} + C_m\Psi_{2,-1}, \tag{3.33}$$

where ϕ_m^* given by (3.31) is a special solution of the mth-order deformation equations (3.24)–(3.27), and A_m, B_m, C_m are constants to be determined.

Obviously, according to (3.30), the solution of the high-order deformation equations (3.24)–(3.27) has secular terms when the right-hand side of (3.25) contains the terms $\sin\xi_1$, $\sin\xi_2$ and $\sin(2\xi_1 - \xi_2)$. This is exactly the mathematical reason why the wave amplitude of a resonant wave given by perturbation methods grows linearly with time. Fortunately, the HAM gives us great freedom in the choice of the initial guess solution $\phi_0(\xi_1, \xi_2, z)$, so we can choose the initial guess

$$\phi_0(\xi_1, \xi_1, z) = A_0\Psi_{1,0} + B_0\Psi_{0,1} + C_0\Psi_{2,-1}, \tag{3.34}$$

where A_0, B_0 and C_0 are unknown constants, which are determined by avoiding the above-mentioned secular terms, as shown later. Note that the above initial guess ϕ_0 automatically satisfies the governing equation (2.13) and the bottom condition (2.16) for arbitrary values of A_0, B_0, C_0.

Note that, from the viewpoint of perturbation methods, (3.34) implies that the resonant wave is of the same order as the primary waves. In fact, if the resonant component is neglected in (3.34), it is impossible to obtain steady-state resonant solutions. This is exactly the mathematical reason why Phillips (1960, 1981) obtained the so-called resonant waves with linearly increasing wave amplitude. Fortunately, since the HAM is independent of small/large physical parameters, we need not consider the orders of different wave components at all.

4. Steady-state resonant waves for $\alpha_2 = \pi/36$

Without loss of generality, let us first consider the following particular case:

$$\frac{\sigma_1}{\omega_1} = \frac{\sigma_2}{\omega_2} = \epsilon, \quad \alpha_1 = 0, \quad \alpha_2 = \frac{\pi}{36}. \tag{4.1}$$

Here, the value of ϵ is slightly larger than 1, since Phillips' criterion (3.32) is valid only for small-amplitude waves.

Substituting all of these parameters into Phillips' criterion (3.32), we have the following nonlinear algebraic equation:

$$\begin{aligned} &-\frac{49}{4}\sqrt{4\left[\frac{(k_1d)}{(k_2d)}\right]^2 + 1 - 4\frac{(k_1d)}{(k_2d)}\cos(\alpha_2-\alpha_1)} \\ &\times \tanh\left[(k_2d)\sqrt{4\left[\frac{(k_1d)}{(k_2d)}\right]^2 + 1 - 4\frac{(k_1d)}{(k_2d)}\cos(\alpha_2-\alpha_1)}\right] \\ &+\frac{196}{5}\frac{(k_1d)}{(k_2d)}\tanh(k_1d) + \frac{49}{5}\tanh(k_2d) \\ &-\frac{196}{5}\sqrt{\frac{(k_1d)}{(k_2d)}\tanh(k_1d)}\sqrt{\tanh(k_2d)} = 0. \end{aligned} \tag{4.2}$$

Without loss of generality, let us first consider the case of $\epsilon = 1.0003$ and $k_2d = 3\pi/5$. In this case, (4.2) has three solutions, $k_1d = 2.06269$, 1.69564 and 0.867072, respectively, corresponding to three resonance states with $k_2/k_1 = 0.913835$, 1.11165 and 2.173797, labelled A, B and C in figure 1. Obviously, for different k_2d and ϵ, the ratios of k_2/k_1 for the corresponding fully resonant waves are different, as listed in table 1. Note that k_2/k_1 of resonance state A is always less than 1, k_2/k_1 of resonance state B is always greater than 1 but less than 2, k_2/k_1 of resonance state C is always

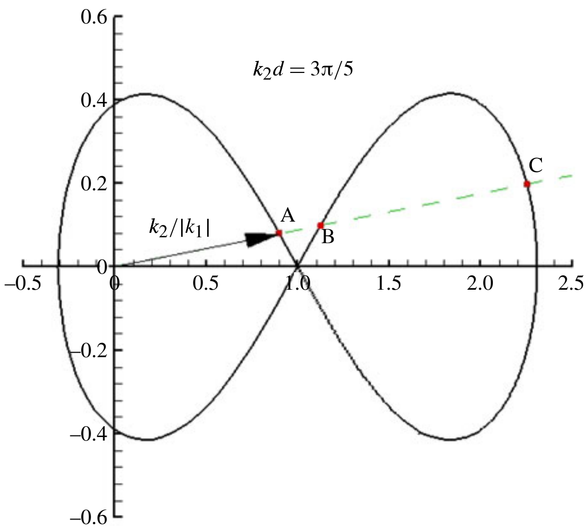

FIGURE 1. (Colour online) Ratio of $\boldsymbol{k}_2/k_1$ for (4.1) with $\epsilon = 1.0003$ and $k_2d = 3\pi/5$ for fully resonant waves.

k_2d	Resonance state		
	A	B	C
$\pi/2$	0.915363	1.114412	2.127085
$3\pi/5$	0.913835	1.111651	2.173797
$7\pi/10$	0.910292	1.112974	2.209941
$4\pi/5$	0.906069	1.116521	2.237180
$9\pi/10$	0.902109	1.121135	2.257012
π	0.898910	1.126032	2.270822
$13\pi/10$	0.893996	1.138198	2.287568
$3\pi/2$	0.892992	1.142949	2.286638
$17\pi/10$	0.892636	1.145541	2.281206
$21\pi/10$	0.892479	1.147408	2.265765
3π	0.892462	1.147851	2.235292
$+\infty$	0.892461	1.147859	2.196364

TABLE 1. Ratios of k_2/k_1 for the three different resonance states for (4.1) with various k_2d when Phillips' resonance criterion (3.32) is exactly satisfied. The values of A, B and C are obtained by means of $k_2 = \pi/5$ (m^{-1}) and the corresponding values of d.

greater than 2, respectively. Note also that resonance states B and C in table 1 were neglected by Liao (2011) for steady-state fully resonant waves in deep water.

4.1. *Steady-state fully resonant waves for resonance state A*

Without loss of generality, we first take $k_2/k_1 = 0.913835$ for (4.1) with $k_2d = 3\pi/5$ as an example, corresponding to resonance state A, to illustrate the above-mentioned analytic approach in detail.

Since Phillips' resonance criterion (3.32) is fully satisfied, there are three zero eigenvalues $\lambda_{1,0}$, $\lambda_{0,1}$ and $\lambda_{2,-1}$, as mentioned above. Thus, according to (3.30), the coefficients of the terms $\sin\xi_1$, $\sin\xi_2$ and $\sin(2\xi_1 - \xi_2)$ on the right-hand side of (3.25)

A_0	B_0	C_0
	Group A1	
−0.061834	0.043603	−0.0866169
−0.061834	−0.043603	0.0866169
0.061834	0.043603	−0.0866169
0.061834	−0.043603	0.0866169
	Group A2	
−0.0616515	−0.0582749	−0.0435411
−0.0616515	0.0582749	0.0435411
0.0616515	−0.0582749	−0.0435411
0.0616515	0.0582749	0.0435411
	Group A3	
−0.0616228	0.115536	−0.0326345
−0.0616228	−0.115536	0.0326345
0.0616228	0.115536	−0.0326345
0.0616228	−0.115536	0.0326345

TABLE 2. Solutions of the nonlinear algebraic equations (4.4)–(4.6) when $k_2/k_1 = 0.913835$ (corresponding to resonance state A) for (4.1) with $\epsilon = 1.0003$ and $k_2 d = 3\pi/5$. The values of A_0, B_0 and C_0 are obtained by means of $k_2 = \pi/5$ (m^{-1}) and $d = 3$ (m).

must be zero so as to avoid the secular terms, because they do not satisfy the solution expression (2.19). For example, substituting the initial guess (3.34) into the first-order deformation equation (3.25), we have

$$
\begin{aligned}
\bar{\mathscr{L}}[\phi_1] &= c_0 \Delta_0^{\phi} - \bar{S}_1 \\
&= \tilde{b}_{1,0} \sin \xi_1 + \tilde{b}_{0,1} \sin \xi_2 + \tilde{b}_{2,0} \sin 2\xi_1 + \tilde{b}_{0,2} \sin 2\xi_2 \\
&\quad + \tilde{b}_{1,-1} \sin(\xi_1 - \xi_2) + \tilde{b}_{1,1} \sin(\xi_1 + \xi_2) \\
&\quad + \tilde{b}_{1,2} \sin(\xi_1 + 2\xi_2) + \tilde{b}_{3,0} \sin 3\xi_1 + \tilde{b}_{0,3} \sin 3\xi_2 \\
&\quad + \tilde{b}_{1,-2} \sin(\xi_1 - 2\xi_2) + \tilde{b}_{2,-1} \sin(2\xi_1 - \xi_2) \\
&\quad + \tilde{b}_{3,-1} \sin(3\xi_1 - \xi_2) + \tilde{b}_{2,-2} \sin(2\xi_1 - 2\xi_2) \\
&\quad + \tilde{b}_{2,-3} \sin(2\xi_1 - 3\xi_2) + \tilde{b}_{3,-2} \sin(3\xi_1 - 2\xi_2) \\
&\quad + \tilde{b}_{2,1} \sin(2\xi_1 + \xi_2) + \tilde{b}_{4,-1} \sin(4\xi_1 - \xi_2) \\
&\quad + \tilde{b}_{4,-2} \sin(4\xi_1 - 2\xi_2) + \tilde{b}_{4,-3} \sin(4\xi_1 - 3\xi_2) \\
&\quad + \tilde{b}_{5,-2} \sin(5\xi_1 - 2\xi_2) + \tilde{b}_{6,-3} \sin(6\xi_1 - 3\xi_2),
\end{aligned} \tag{4.3}
$$

where $\tilde{b}_{m,n}$ depends upon the three unknown coefficients A_0, B_0 and C_0 of the initial guess (3.34). According to (3.30), we must enforce $\tilde{b}_{1,0} = 0$, $\tilde{b}_{0,1} = 0$ and $\tilde{b}_{2,-1} = 0$ to avoid secular terms, which gives us a set of three nonlinear algebraic equations:

$$-0.00391489 + 0.206A_0^2 + 0.307855B_0^2 + 0.413579B_0C_0 + 0.547011C_0^2 = 0, \tag{4.4}$$

$$-0.00352853 + 0.372512A_0^2 + 0.13869B_0^2 + 0.247221A_0^2C_0/B_0 + 0.495605C_0^2 = 0, \tag{4.5}$$

$$0.16962A_0^2B_0 - 0.0043213C_0 + 0.45485A_0^2C_0 + 0.341129B_0^2C_0 + 0.301249C_0^3 = 0. \tag{4.6}$$

This set of nonlinear algebraic equations (4.4)–(4.6) has 12 solutions with real values, as listed in table 2. Each of them corresponds to a steady-state fully resonant wave system, as shown later. They can be divided into three groups called A1, A2 and A3: each group has the same values of $|A_0|$, $|B_0|$ and $|C_0|$. Note that, for a steady-state fully resonant wave system with the wave elevation in the form (2.12), the wave energy spectrum is determined by the square of wave components, i.e. $a_{m,n}^2$, and is therefore independent of time. Thus, the three initial guesses $\phi_0(\xi_1, \xi_2, z)$ in the same group lead to the same time-independent spectrum of wave energy. Indeed, our computations based on the convergent analytic series indicate that the waves given by different initial guess $\phi_0(\xi_1, \xi_2, z)$ in the same group have the same wave energy spectrum, as shown later. Therefore, it is necessary for us to investigate only one case of A_0, B_0 and C_0 in each group.

As long as A_0, B_0 and C_0 are determined, the initial guess $\phi_0(\xi_1, \xi_2, z)$ is known. Then, substituting this known ϕ_0 into (3.26), we can directly obtain $\eta_1(\xi_1, \xi_2)$. Note that from now on the right-hand side of (4.3) does not contain the terms $\sin\xi_1$, $\sin\xi_2$ and $\sin(2\xi_1 - \xi_2)$. So, using (3.30), it is straightforward to obtain

$$\phi_1 = \phi_1^* + A_1\Psi_{1,0} + B_1\Psi_{0,1} + C_1\Psi_{2,-1}, \tag{4.7}$$

where A_1, B_1 and C_1 are unknown constant coefficients, and

$$\begin{aligned}\phi_1^* = {} & \tilde{d}_{2,0}\Psi_{2,0} + \tilde{d}_{3,0}\Psi_{3,0} \\ & + \tilde{d}_{2,-3}\Psi_{2,-3} + \tilde{d}_{4,-3}\Psi_{4,-3} + \tilde{d}_{6,-3}\Psi_{6,-3} + \tilde{d}_{1,-2}\Psi_{1,-2} + \tilde{d}_{2,-2}\Psi_{2,-2} \\ & + \tilde{d}_{3,-2}\Psi_{3,-2} + \tilde{d}_{4,-2}\Psi_{4,-2} + \tilde{d}_{5,-2}\Psi_{5,-2} + \tilde{d}_{1,-1}\Psi_{1,-1} + \tilde{d}_{3,-1}\Psi_{3,-1} \\ & + \tilde{d}_{4,-1}\Psi_{4,-1} + \tilde{d}_{0,2}\Psi_{0,2} + \tilde{d}_{0,3}\Psi_{0,3} + \tilde{d}_{1,1}\Psi_{1,1} + \tilde{d}_{2,1}\Psi_{2,1} + \tilde{d}_{1,2}\Psi_{1,2}\end{aligned} \tag{4.8}$$

is a special solution with the definition $\tilde{d}_{m,n} = \tilde{b}_{m,n}/\lambda_{m,n}$. Here, the eigenvalue $\lambda_{m,n}$ is given by (3.23). So, using a computer algebra system such as Mathematica or Maple, it is rather easy to obtain η_1 and ϕ_1 in this way.

When $m \geqslant 2$, the unknown coefficients A_{m-1}, B_{m-1} and C_{m-1} in the common solution (3.33) can be obtained by avoiding the secular terms in a similar way, except that they are determined by a set of linear algebraic equations. As long as A_{m-1}, B_{m-1} and C_{m-1} are known, we can obtain $\eta_m(\xi_1, \xi_2)$ and $\phi_m(\xi_1, \xi_2, z)$ in a similar way. All of this can be done efficiently by means of Mathematica or Maple. Thus, we can obtain the high-order approximations of the velocity potential $\phi(\xi_1, \xi_2, z)$ and the wave elevation $\eta(\xi_1, \xi_2)$ efficiently.

It should be emphasized that the so-called convergence-control parameter c_0, which is used to guarantee the convergence of our approximations, is still unknown at this point. The optimal value of c_0 corresponds to the fastest decrease of the averaged residual squares ε_m^ϕ and ε_m^η of the two free-surface boundary conditions, defined by

$$\varepsilon_m^\phi = \frac{1}{(1+M)^2}\sum_{i=0}^{M}\sum_{j=0}^{M}\left[\sum_{n=0}^{m}\Delta_n^\phi(i\,\triangle\,\xi_1, j\,\triangle\,\xi_2)\right]^2, \tag{4.9}$$

$$\varepsilon_m^\eta = \frac{1}{(1+M)^2}\sum_{i=0}^{M}\sum_{j=0}^{M}\left[\sum_{n=0}^{m}\Delta_n^\eta(i\,\triangle\,\xi_1, j\,\triangle\,\xi_2)\right]^2, \tag{4.10}$$

respectively, where Δ_n^ϕ and Δ_n^η are given in appendix A, M is the number of the discrete points, and

$$\triangle\xi_1 = \triangle\xi_2 = \frac{\pi}{M}. \tag{4.11}$$

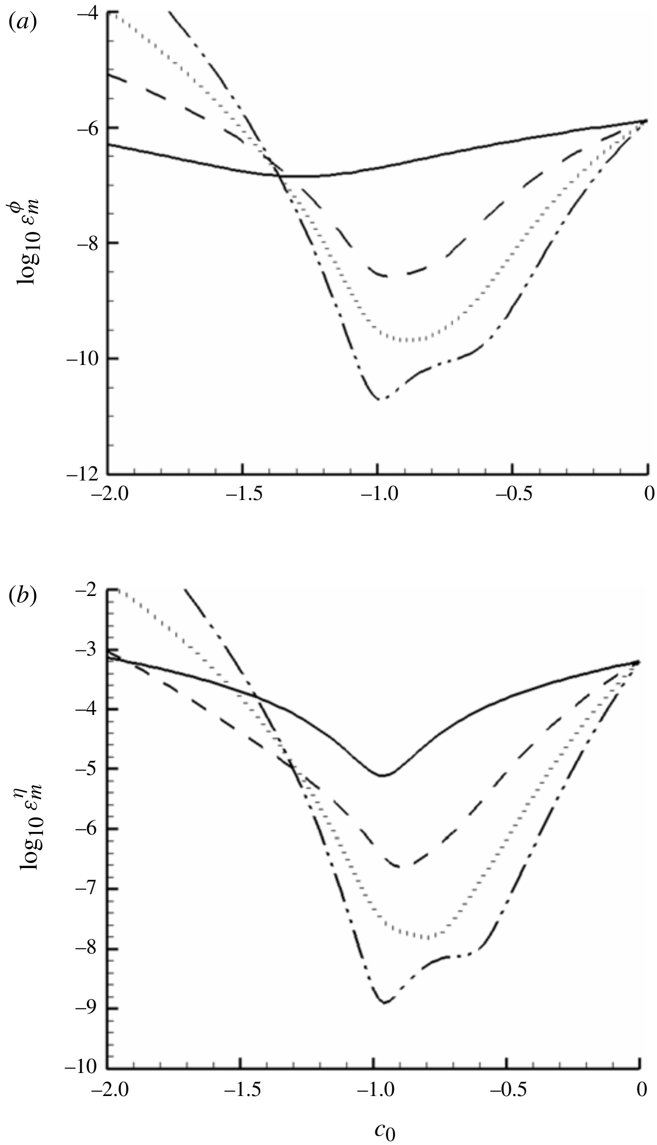

FIGURE 2. Residual squares of $\log_{10}\varepsilon_m^{\phi}$ and $\log_{10}\varepsilon_m^{\eta}$ versus c_0 for (4.1) with $\epsilon = 1.0003$, $k_2/k_1 = 0.913835$ and $k_2 d = 3\pi/5$ when $A_0 = -0.061834$, $B_0 = 0.043603$ and $C_0 = -0.0866169$ (corresponding to group A1). Solid line, first-order approximation; dashed line, third-order approximation; dotted line, fifth-order approximation; dash-dot-dotted line, seventh-order approximation.

A convergence theorem given by Liao (2003) (Theorem 2.1) guarantees the rationality of (4.9) and (4.10). In this paper, $M = 10$ is used. For example, when $A_0 = -0.061834$, $B_0 = 0.043603$ and $C_0 = -0.0866169$, corresponding to group A1, the averaged residual squares ε_m^{ϕ} and ε_m^{η} at different orders of approximation are as shown in figure 2. It is found that the residual squares of two free-surface boundary conditions have the smallest values around $c_0 = -0.98$. So, we choose the optimal convergence-

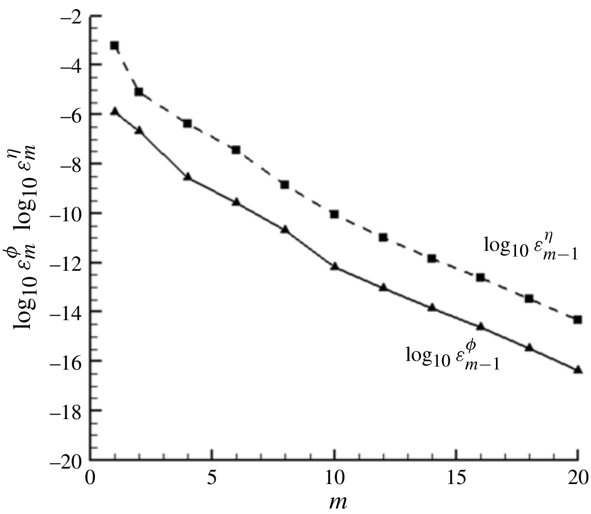

FIGURE 3. Residual squares of $\log_{10}\varepsilon_m^{\phi}$ and $\log_{10}\varepsilon_m^{\eta}$ versus the approximation order m for (4.1) with $\epsilon = 1.0003$, $k_2/k_1 = 0.913835$ and $k_2d = 3\pi/5$ when $A_0 = -0.061834$, $B_0 = 0.043603$ and $C_0 = -0.0866169$ (corresponding to group A1) by means of $c_0 = -0.98$. Solid line, $\log_{10}\varepsilon_m^{\phi}$; dashed line, $\log_{10}\varepsilon_m^{\eta}$.

Order of approx.	Amplitude of wave component			Residual squares	
m	$\lvert a_{1,0}\rvert/d$	$\lvert a_{0,1}\rvert/d$	$\lvert a_{2,-1}\rvert/d$	ε_{m-1}^{ϕ}	ε_{m-1}^{η}
2	0.004115	0.003560	0.008845	2.05×10^{-7}	7.80×10^{-6}
6	0.003738	0.003251	0.008790	2.66×10^{-10}	3.60×10^{-8}
10	0.003743	0.003268	0.008782	6.61×10^{-13}	8.74×10^{-11}
14	0.003739	0.003269	0.008782	1.40×10^{-14}	1.44×10^{-12}
18	0.003739	0.003269	0.0087817	3.38×10^{-16}	3.49×10^{-14}
20	0.003739	0.003269	0.0087817	4.41×10^{-17}	4.89×10^{-15}

TABLE 3. The mth-order approximation of $|a_{1,0}|/d$, $|a_{0,1}|/d$ and $|a_{2,-1}|/d$ by means of $c_0 = -0.98$, together with the corresponding residual square ε_{m-1}^{ϕ} and ε_{m-1}^{η} for (4.1) with $\epsilon = 1.0003$, $k_2d = 3\pi/5$ and $k_2/k_1 = 0.913835$ (corresponding to resonance state A) when $A_0 = -0.061834$, $B_0 = 0.043603$ and $C_0 = -0.0866169$ (corresponding to group A1).

control parameter $c_0 = -0.98$. Using this optimal value of c_0, the two averaged residual squares decrease rather quickly, as shown in table 3 and figure 3. Note that, at the 20th order of approximation, the averaged residual squares of the two free-surface boundary conditions decrease to the level of 10^{-17} and 10^{-15}, respectively, which indicates, without doubt, the convergence of our approximation. Note also that the approximations of the amplitudes $a_{0,1}$, $a_{1,0}$, $a_{2,-1}$ of the two primary waves $\cos\xi_1$, $\cos\xi_2$ and the resonant wave component $\cos(2\xi_1 - \xi_2)$ converge quickly, as shown in table 3.

Similarly, we obtain the convergent velocity potential and wave elevation for group A2 by means of $c_0 = -1$ and for group A3 by means of $c_0 = -1.15$. The corresponding wave amplitudes of the primary and resonant wave components are

	Amplitude of wave components (Primary wave) $\lvert a_{1,0}\rvert/d$	(Primary wave) $\lvert a_{0,1}\rvert/d$	(Resonant wave) $\lvert a_{2,-1}\rvert/d$
Group A1	0.003739	0.003269	0.008782
Group A2	0.005275	0.003745	0.005110
Group A3	0.006657	0.007922	0.003068

TABLE 4. Amplitude of wave components $|a_{1,0}|/d$, $|a_{0,1}|/d$ and $|a_{2,-1}|/d$ for (4.1) when $\epsilon = 1.0003$, $k_2 d = 3\pi/5$ and $k_2/k_1 = 0.913835$ (corresponding to resonance state A). Group A1, $A_0 = -0.061834$, $B_0 = 0.043603$, $C_0 = -0.0866169$ and $c_0 = -0.98$; group A2, $A_0 = -0.0616515$, $B_0 = -0.0582749$, $C_0 = -0.0435411$ and $c_0 = -1$; group A3, $A_0 = -0.0616228$, $B_0 = 0.115536$, $C_0 = -0.0326345$ and $c_0 = -1.15$.

	Distribution of wave energy (Primary wave) $a_{1,0}^2/\Pi$ (%)	(Primary wave) $a_{0,1}^2/\Pi$ (%)	(Resonant wave) $a_{2,-1}^2/\Pi$ (%)	Sum Π_0/Π (%)
Group A1	13.72	10.48	75.64	99.84
Group A2	40.43	20.38	37.93	98.74
Group A3	37.80	53.54	8.03	99.37

TABLE 5. Wave energy distribution for different groups of steady-state fully resonant wave systems for (4.1) when $\epsilon = 1.0003$, $k_2 d = 3\pi/5$ and $k_2/k_1 = 0.913835$ (corresponding to resonance state A).

listed in table 4. The wave energy distributions for the three groups of waves are given in table 5, where Π_0 denotes the sum of wave energy of the two primary and one resonant wave components, and Π is the total wave energy of the entire wave system, defined by

$$\Pi_0 = a_{1,0}^2 + a_{0,1}^2 + a_{2,-1}^2, \quad \Pi = \sum_{m=0}^{+\infty} \sum_{n=-\infty}^{+\infty} a_{m,n}^2, \tag{4.12}$$

respectively.

Now we immediately obtain the solutions of the three groups of the steady-state fully resonant waves for (4.1) with $\epsilon = 1.0003$ and $k_2 d = 3\pi/5$ for resonance state A. It is found that the two primary and one resonant wave components as a whole contain $\sim$99 % of the wave energy, and thus all other wave components are negligible. Note that the resonant wave amplitude $a_{2,-1}$ is of the same order as that of the two primary ones, i.e.

$$O(a_{2,-1}) = O(a_{0,1}) = O(a_{1,0}), \tag{4.13}$$

as shown in table 4. This agrees well with the conclusions given by Benney (1962). Note that the steady-state resonant wave in group A1 contains the largest proportion (75.64 %) of the wave energy. However, the resonant wave component does not always contain the largest proportion of the wave energy for a steady-state wave system: for example, the resonant wave in group A2 contains only 37.93 % of the wave energy, which is a little less than that of one of the primary ones (40.43 %) but greater than that of the other (20.38 %). In particular, the resonant wave in group A3 contains the smallest proportion (8.03 %) of the wave energy, which is much less than those of

$k_2 d$	Proportion of wave energy (Primary wave) $a_{1,0}^2/\Pi$ (%)	(Primary wave) $a_{0,1}^2/\Pi$ (%)	(Resonant wave) $a_{2,-1}^2/\Pi$ (%)	Sum Π_0/Π (%)
$3\pi/5$	13.71	10.48	75.64	99.84
$7\pi/10$	12.76	10.71	76.29	99.76
$4\pi/5$	12.03	10.93	76.75	99.71
$9\pi/10$	11.57	11.12	77.01	99.70
π	11.32	11.28	77.11	99.71
$13\pi/10$	11.12	11.62	77.02	99.76
$3\pi/2$	11.11	11.75	76.91	99.77
$17\pi/10$	11.11	11.84	76.82	99.77
$21\pi/10$	11.09	11.97	76.71	99.77
3π	11.00	12.14	76.62	99.76
$33\pi/10$	10.98	13.2	76.61	99.76
∞	10.88	12.29	76.58	99.76

TABLE 6. Wave energy distribution for group A1 for (4.1) with $\epsilon = 1.0003$ and various $k_2 d$. The corresponding values of k_2/k_1 are given in resonance state A in table 1.

$k_2 d$	Proportion of wave energy (Primary wave) $a_{1,0}^2/\Pi$ (%)	(Primary wave) $a_{0,1}^2/\Pi$ (%)	(Resonant wave) $a_{2,-1}^2/\Pi$ (%)	Sum Π_0/Π (%)
$3\pi/5$	40.43	20.38	37.94	98.74
$7\pi/10$	39.77	19.47	38.95	98.19
$4\pi/5$	39.37	18.84	39.62	97.83
$9\pi/10$	39.27	18.50	39.97	97.74
π	39.36	18.38	40.10	97.83
$13\pi/10$	39.74	18.44	40.00	98.18
$3\pi/2$	39.88	18.51	39.88	98.27
$17\pi/10$	39.95	18.55	39.80	98.30
$21\pi/10$	40.04	18.58	39.70	98.31
3π	40.12	18.57	39.61	98.30
$33\pi/10$	40.14	18.57	39.59	98.30
∞	40.17	18.54	39.56	98.27

TABLE 7. Wave energy distribution for group A2 for (4.1) with $\epsilon = 1.0003$ and various $k_2 d$. The corresponding values of k_2/k_1 are given in resonance state A in table 1.

the two primary ones (37.8 % and 53.54 %), as shown in table 5. Therefore, steady-state resonant waves also exist in finite water depth, and, further, the resonant wave components can contain only a small proportion of the total wave energy. So, the conclusions given by Liao (2011) for steady-state fully resonant waves in deep water have general application.

Unlike Liao (2011), we consider in this article the steady-state resonant waves in finite water depth. So, the effect of water depth is studied here in detail. It is found that, in resonance state A, there always exist three different groups of steady-state fully resonant waves in different water depths, called group Ai ($i = 1, 2, 3$). The wave energy distributions of the two primary and one resonant components of the three groups in different water depths are shown in figure 4 and tables 6–8. It is found that the resonant wave component in group A1 always contains the largest proportion of the wave energy, but that of group A3 always contains the smallest ones.

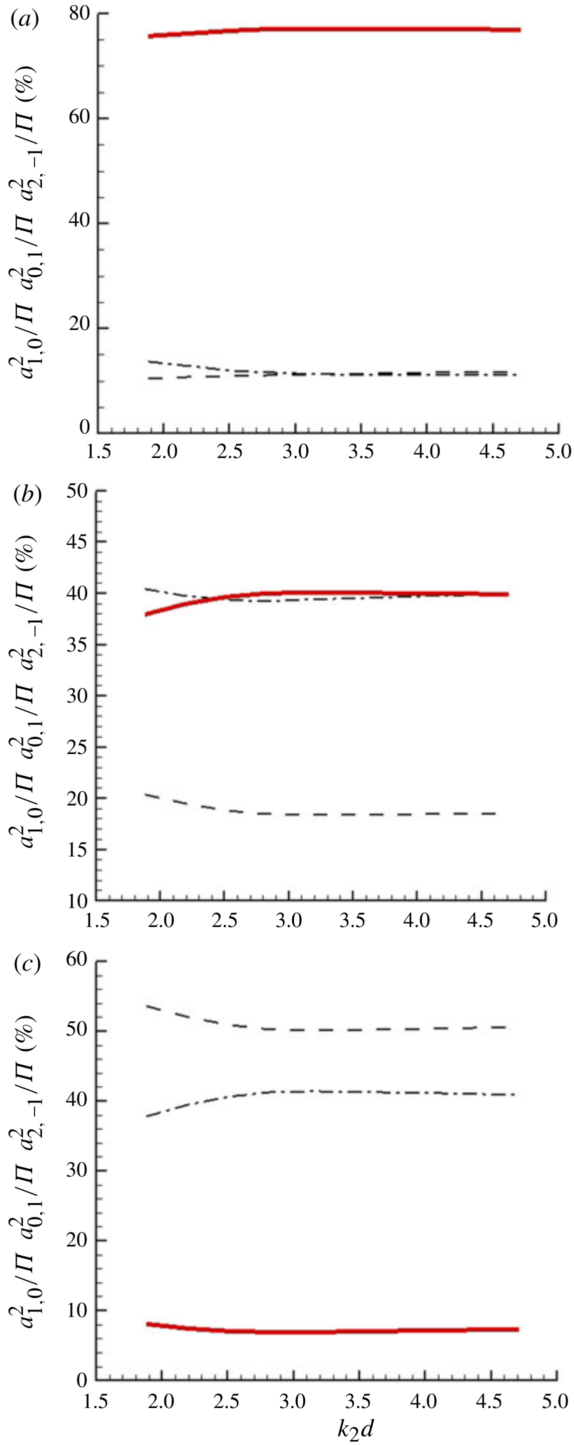

FIGURE 4. (Colour online) Wave energy distribution for (4.1) with $\epsilon = 1.0003$ and various k_2d for resonance state A in table 1. (*a*) Group A1, (*b*) group A2, (*c*) group A3. Dash-dotted line, $a^2_{1,0}/\Pi$ (first primary wave); dashed line, $a^2_{0,1}/\Pi$ (second primary wave); solid line, $a^2_{2,-1}/\Pi$ (resonant wave).

k_2d	Proportion of wave energy (Primary wave) $a^2_{1,0}/\Pi$ (%)	(Primary wave) $a^2_{0,1}/\Pi$ (%)	(Resonant wave) $a^2_{2,-1}/\Pi$ (%)	Sum Π_0/Π (%)
$3\pi/5$	37.80	53.54	8.03	99.37
$7\pi/10$	39.49	51.99	7.46	98.94
$4\pi/5$	40.66	50.85	7.07	98.58
$9\pi/10$	41.26	50.27	6.94	98.47
π	41.44	50.12	6.98	98.54
$13\pi/10$	41.18	50.37	7.25	98.80
$3\pi/2$	40.92	50.59	7.36	98.87
$17\pi/10$	40.72	50.74	7.42	98.88
$21\pi/10$	40.45	50.93	7.49	98.88
3π	40.16	51.11	7.59	98.86
$33\pi/10$	40.10	51.14	7.61	98.85
∞	39.97	51.19	7.65	98.82

TABLE 8. Wave energy distribution for group A3 for (4.1) with $\epsilon = 1.0003$ and various k_2d. The corresponding values of k_2/k_1 are given in resonance state A in table 1.

Based on our above-mentioned results, in resonance state A listed in table 1 there do indeed always exist multiple steady-state fully resonant waves in water of finite depth. Moreover, the amplitude of the resonant wave component is of the same order as those of the two primary ones, and the two primary and one resonant wave components as a whole contain nearly 99 % of the wave energy. Furthermore, for steady-state resonant waves in finite water depth, the resonant wave component can contain a much smaller proportion of the wave energy than the primary ones. Note that the same conclusions were reported by Liao (2011) for steady-state fully resonant waves in deep water. So, in this subsection, we further verify that Liao's conclusions still hold in finite water depth for resonance state A and thus have general application.

4.2. *Steady-state fully resonant waves in resonance state B*

As shown in table 1, when Phillips' resonance criterion is exactly satisfied, there exist three steady-state resonance states for (4.1) with $\epsilon = 1.0003$ but different k_2d: $k_2/k_1 < 1$ for resonance state A, $1 < k_2/k_1 < 2$ for resonance state B and $k_2/k_1 > 2$ for resonance state C. Note that resonance states B and C were neglected by Liao (2011) for steady-state fully resonant waves in deep water. In this subsection, we focus on resonance state B.

Similarly, we first take $k_2d = 3\pi/5$ as an example of resonance state B. The analytic approach is exactly the same as that described in § 4.1, and is thus omitted here. To avoid the secular terms, we have a set of the nonlinear algebra equations

$$-0.003107 + 0.0859796A_0^2 + 0.245246B_0^2 + 0.172718B_0C_0 + 0.11889C_0^2 = 0, \quad (4.14)$$

$$-0.0035285 + 0.1951A_0^2 + 0.13869B_0^2 + 0.0673168A_0^2C_0/B_0 + 0.13566C_0^2 = 0, \quad (4.15)$$

$$0.1078A_0^2B_0 - 0.002713C_0 + 0.151046A_0^2C_0 + 0.21599B_0^2C_0 + 0.0519C_0^3 = 0, \quad (4.16)$$

which have 12 solutions with real values. As listed in table 9, they can be divided into three groups, denoted by groups B1, B2 and B3, respectively, and each group contains four different solutions but the same values of $|A_0|$, $|B_0|$ and $|C_0|$.

Again, choosing an optimal convergent-control parameter c_0, we obtain the convergent analytic approximations for groups B1, B2 and B3, as shown in table 10.

A_0	B_0	C_0
	Group B1	
−0.0847735	0.0431112	−0.165801
−0.0847735	−0.0431112	0.165801
0.0847735	0.0431112	−0.165801
0.0847735	−0.0431112	0.165801
	Group B2	
−0.0850092	−0.057744	−0.0837223
−0.0850092	0.057744	0.0837223
0.0850092	−0.057744	−0.0837223
0.0850092	0.057744	0.0837223
	Group B3	
−0.0855548	0.115225	−0.0622215
−0.0855548	−0.115225	0.0622215
0.0855548	0.115225	−0.0622215
0.0855548	−0.115225	0.0622215

TABLE 9. Solutions of A_0, B_0, C_0 of the nonlinear algebraic equations (4.14)–(4.16) for (4.1) when $\epsilon = 1.0003$, $k_2 d = 3\pi/5$ and $k_2/k_1 = 1.11165$ (corresponding to resonance state B). The values of A_0, B_0 and C_0 are obtained by means of $k_2 = \pi/5$ (m^{-1}) and $d = 3$ (m).

	Amplitude of wave components		
	(Primary wave) $\lvert a_{1,0}\rvert/d$	(Primary wave) $\lvert a_{0,1}\rvert/d$	(Resonant wave) $\lvert a_{2,-1}\rvert/d$
Group B1	0.007858	0.0038778	0.009394
Group B2	0.006488	0.0060748	0.004662
Group B3	0.004382	0.010358	0.003832

TABLE 10. Convergent amplitude ($\lvert a_{1,0}\rvert/d$, $\lvert a_{0,1}\rvert/d$ and $\lvert a_{2,-1}\rvert/d$) of some wave components for (4.1) when $\epsilon = 1.0003$, $k_2 d = 3\pi/5$ and $k_2/k_1 = 1.11165$ (corresponding to resonance state B).

Thus, for (4.1) with $\epsilon = 1.0003$, $k_2 d = 3\pi/5$ and $k_2/k_1 = 1.11165$ (corresponding to resonance state B), there also exist three steady-state fully resonant waves which have no exchange of wave energy between different wave modes, so the wave spectrum is independent of time. Further, the resonant wave component may also contain a much smaller proportion of the wave energy than that of the primary ones, as shown in table 11 (see groups B2 and B3). This confirms our conclusions described in § 4.1 concerning steady-state fully resonant waves for resonance state A. Note that, unlike resonance state A in § 4.1, the resonant component in group B1 shares only 53.45 % of the wave energy of the entire wave system, while the counterpart in § 4.1 for group A1 has a much larger proportion, i.e. 75.64 %. In addition, one primary wave in group B3 contains 76.05 % of the wave energy, which is larger than the counterpart (53.54 %) in § 4.1 for group A3. In particular, the resonant wave component in groups B2 and B3 contains a smaller proportion of the wave energy than that of the two primary ones. Obviously, the steady-state fully resonant waves for resonance state B are quantitatively different from those for resonance state A. However, qualitatively speaking, they yield the same conclusion: there exist multiple

	Distribution of wave energy			Sum
	(Primary wave) $a_{1,0}^2/\Pi$ (%)	(Primary wave) $a_{0,1}^2/\Pi$ (%)	(Resonant wave) $a_{2,-1}^2/\Pi$ (%)	Π_0/Π (%)
Group B1	37.37	9.07	53.45	99.89
Group B2	41.67	36.53	21.51	99.72
Group B3	13.51	76.05	10.40	99.95

TABLE 11. Wave energy distribution of the three steady-state fully resonant waves for (4.1) when $\epsilon = 1.0003$, $k_2 d = 3\pi/5$ and $k_2/k_1 = 1.11165$ (corresponding to resonance state B).

$k_2 d$	Proportion of wave energy			Sum
	(Primary wave) $a_{1,0}^2/\Pi$ (%)	(Primary wave) $a_{0,1}^2/\Pi$ (%)	(Resonant wave) $a_{2,-1}^2/\Pi$ (%)	Π_0/Π (%)
$3\pi/5$	37.37	9.07	53.45	99.89
$7\pi/10$	38.01	8.64	53.16	99.82
$4\pi/5$	39.32	8.36	52.05	99.73
$9\pi/10$	40.45	8.16	51.05	99.66
π	41.35	8.04	50.22	99.61
$13\pi/5$	42.89	8.06	48.71	99.66
$3\pi/2$	43.26	8.15	48.30	99.71
$17\pi/10$	43.32	8.23	48.18	99.73
$21\pi/10$	43.08	8.35	48.32	99.75
3π	42.57	8.47	48.70	99.75
$33\pi/10$	42.48	8.50	48.77	99.75
∞	42.19	8.58	48.98	99.75

TABLE 12. Wave energy distribution for group B1 for (4.1) with $\epsilon = 1.0003$ and various $k_2 d$. The corresponding values of k_2/k_1 are given in resonance state B in table 1.

steady-state fully resonant waves whose resonant wave component can contain only a small proportion of the wave energy.

The wave energy distributions of three steady-state fully resonant waves in different water depth d are as shown in figure 5 and in tables 12–14, where group Bi ($i = 1, 2, 3$) denotes the ith group of steady-state fully resonant waves in various water depths for resonance state B. It is found that there always exist three steady-state fully resonant waves, and that the resonant wave component may also contain much less wave energy than the primary ones. This confirms that our conclusions given in § 4.1 for resonance state A have general application.

4.3. *Steady-state fully resonant waves in resonance state C*

Let us further consider the steady-state fully resonant waves for (4.1) with $\epsilon = 1.0003$, $k_2 d = 3\pi/5$ and $k_2/k_1 = 2.173797$, corresponding to resonance state C in figure 1.

Similarly, to avoid the secular terms, we have a set of nonlinear algebraic equations in the three unknown coefficients of the initial guess (3.34):

$$-0.118972 + 0.252909A_0^2 + 9.45119B_0^2 + 0.51183B_0C_0 - 0.00520192C_0^2 = 0, \quad (4.17)$$

$$-0.352853 + 1.19945A_0^2 + 13.869B_0^2 + 0.037475A_0^2C_0/B_0 - 0.039547C_0^2 = 0, \quad (4.18)$$

$$1.9347A_0^2B_0 - 0.009184C_0 + 0.05405A_0^2C_0 + 0.7807B_0^2C_0 - 5.378 \times 10^{-4}C_0^3 = 0. \quad (4.19)$$

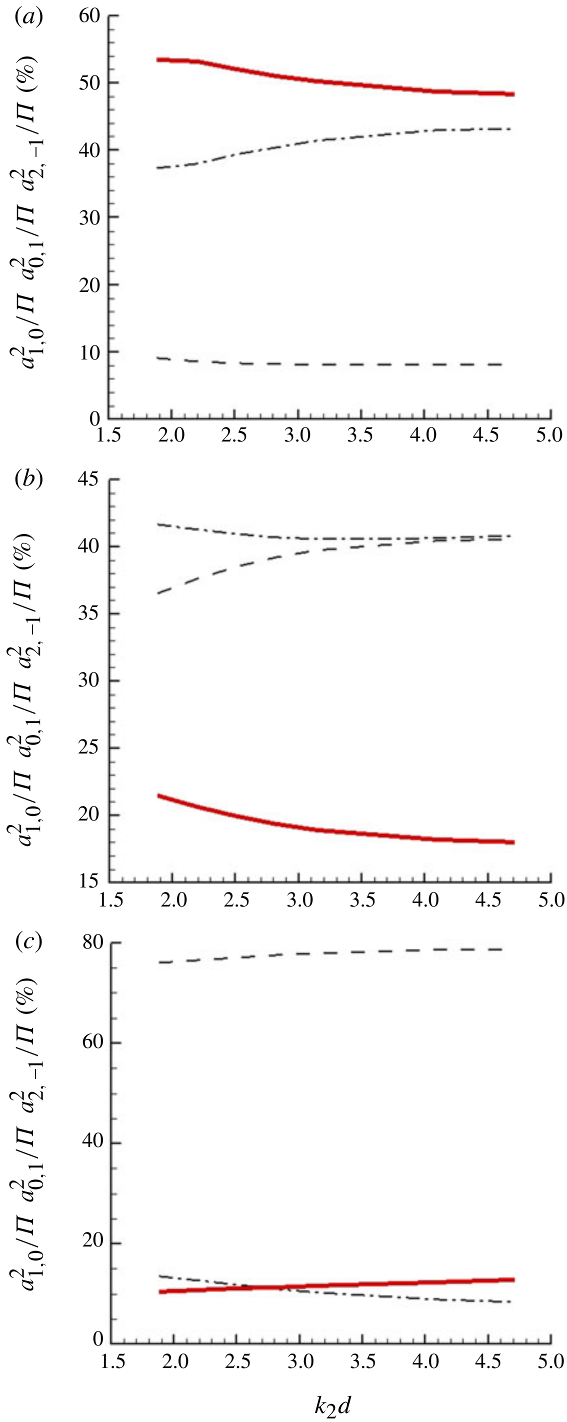

FIGURE 5. (Colour online) Wave energy distribution for (4.1) with $\epsilon = 1.0003$ and various k_2d for resonance state B in table 1. (*a*) Group B1, (*b*) group B2, (*c*) group B3. Dash-dotted line, $a^2_{1,0}/\Pi$ (first primary wave); dashed line, $a^2_{0,1}/\Pi$ (second primary wave); solid line, $a^2_{2,-1}/\Pi$ (resonant wave).

k_2d	Proportion of wave energy (Primary wave) $a^2_{1,0}/\Pi$ (%)	(Primary wave) $a^2_{0,1}/\Pi$ (%)	(Resonant wave) $a^2_{2,-1}/\Pi$ (%)	Sum Π_0/Π (%)
$3\pi/5$	41.67	36.53	21.51	99.71
$7\pi/10$	41.27	37.65	20.65	99.57
$4\pi/5$	40.93	38.53	19.95	99.41
$9\pi/10$	40.68	39.22	19.39	99.29
π	40.55	39.74	18.94	99.23
$13\pi/10$	40.67	40.47	18.18	99.32
$3\pi/2$	40.84	40.58	17.99	99.41
$17\pi/10$	40.98	40.57	17.91	99.46
$21\pi/10$	41.15	40.45	17.90	99.50
3π	41.30	40.27	17.93	99.50
$33\pi/10$	41.33	40.24	17.93	99.50
∞	41.41	40.16	17.93	99.50

TABLE 13. Wave energy distribution for group B2 for (4.1) with $\epsilon = 1.0003$ and various k_2d. The corresponding values of k_2/k_1 are given in resonance state B in table 1.

k_2d	Proportion of wave energy (Primary wave) $a^2_{1,0}/\Pi$ (%)	(Primary wave) $a^2_{0,1}/\Pi$ (%)	(Resonant wave) $a^2_{2,-1}/\Pi$ (%)	Sum Π_0/Π (%)
$3\pi/5$	13.50	76.05	10.40	99.95
$7\pi/10$	12.59	76.57	10.78	99.94
$4\pi/5$	11.78	77.06	11.08	99.92
$9\pi/10$	11.02	77.52	11.37	99.91
π	10.34	77.91	11.66	99.91
$13\pi/10$	8.90	78.62	12.40	99.92
$3\pi/2$	8.39	78.78	12.76	99.93
$17\pi/10$	8.11	78.82	13.00	99.93
$21\pi/10$	7.92	78.73	13.29	99.94
3π	7.81	78.55	13.58	99.94
$33\pi/10$	7.77	78.53	13.64	99.94
∞	7.69	78.44	13.81	99.94

TABLE 14. Wave energy distribution for group B3 for (4.1) with $\epsilon = 1.0003$ and various k_2d. The corresponding values of k_2/k_1 are given in resonance state B in table 1.

The above equations have eight different solutions with real values. They can be divided into two groups (called groups C1 and C2), each containing four different solutions with the same values of $|A_0|$, $|B_0|$ and $|C_0|$, as listed in table 15.

However, using the same HAM-based approach, we cannot obtain convergent analytic approximations by means of these values of A_0, B_0 and C_0 in groups C1 and C2, mainly because there does not exist a so-called convergence-control parameter c_0 such that the convergence of the approximation series can be guaranteed. This is quite different from resonance states A and B, in which it is easy to find the optimal convergence-control parameter c_0 to obtain convergent approximations, as shown for example in figures 2 and 3.

Note that the existence of steady-state fully resonant waves is merely assumed, and our strategy is first to make this assumption and then to prove that the corresponding steady-state fully resonant waves do indeed exist in some cases. If no such steady-state

A_0	B_0	C_0
	Group C1	
−0.586361	−0.0596741	−5.92466
−0.586361	0.0596741	5.92466
0.586361	−0.0596741	−5.92466
0.586361	0.0596741	5.92466
	Group C2	
−0.327547	0.174807	−1.97472
−0.327547	−0.174807	1.97472
0.327547	0.174807	−1.97472
0.327547	−0.174807	1.97472

TABLE 15. Solutions of the nonlinear algebraic equations (4.17)–(4.19) for (4.1) with $\epsilon = 1.0003$, $k_2 d = 3\pi/5$ and $k_2/k_1 = 2.173797$, corresponding to resonance state C in figure 1. The values of A_0, B_0 and C_0 are obtained by means of $k_2 = \pi/5$ (m^{-1}) and $d = 3$ (m).

solutions can be found, this indicates that the assumption is wrong, that is, no steady-state fully resonant waves can exist. Therefore, steady-state fully resonant waves do not exist for (4.1) with $\epsilon = 1.0003$, $k_2 d = 3\pi/5$ and $k_2/k_1 = 2.173797$, corresponding to resonance state C in figure 1.

In summary, for (4.1) with $\epsilon = 1.0003$ and $k_2 d = 3\pi/5$, there exist three resonance states with $k_2/k_1 = 0.913835$ (resonance state A), $k_2/k_1 = 1.11165$ (resonance state B) and $k_2/k_1 = 2.173797$ (resonance state C), respectively, as shown in figure 1 and table 1. Using the HAM-based analytic approach, it is found that, in resonance states A and B, there exist multiple steady-state fully resonant waves and, further, the resonant wave component can contain only a small proportion of the wave energy. However, in resonance state C, such steady-state fully resonant waves do not exist. These conclusions hold for various water depths including deep water. Note that using the famous Zakharov equation we can obtain the same conclusions qualitatively, as shown in appendix B.

5. Steady-state fully resonant waves with different angles between primary waves

As mentioned above, when the angle between the two primary waves is $\pi/36$, there exist multiple steady-state fully resonant waves and, moreover, the resonant wave component can contain only a small proportion of the wave energy, as shown in § 4.1 for resonance state A ($k_2/k_1 < 1$) and in § 4.2 for resonance state B ($1 < k_2/k_1 < 2$). However, no steady-state fully resonant waves are found for resonance state C, as shown in § 4.3. Here, we further illustrate that the these conclusions still hold for some other angles between the two primary waves, and thus have general application.

Without loss of generality, we still consider the case

$$\frac{\sigma_1}{\omega_1} = \frac{\sigma_2}{\omega_2} = 1.0003, \quad \alpha_1 = 0, \quad k_2 d = 3\pi/5, \tag{5.1}$$

as an example. One primary wave propagates in the $\boldsymbol{x}$ direction (i.e. $\alpha_1 = 0$) with unknown magnitude k_1, i.e. $\boldsymbol{k}_1 = k_1 \boldsymbol{i}$. The other has wavenumber $\boldsymbol{k}_2$ with known magnitude but unknown angle α_2. Without loss of generality, we consider two cases, $\alpha_2 = \pi/60$ and $\alpha_2 = 2\pi/45$.

	Distribution of wave energy			Sum
	(Primary wave)	(Primary wave)	(Resonant wave)	
	$a_{1,0}^2/\Pi$ (%)	$a_{0,1}^2/\Pi$ (%)	$a_{2,-1}^2/\Pi$ (%)	Π_0/Π (%)
Group A1	10.85	9.76	77.39	98.00
Group A2	35.06	11.71	41.55	88.32
Group A3	43.76	43.63	3.14	90.53

TABLE 16. Wave energy distribution of steady-state fully resonant waves when $\alpha_1 = 0$, $\alpha_2 = \pi/60$, $\epsilon = 1.0003$, $k_2 d = 3\pi/5$ and $k_2/k_1 = 0.946172$ (resonance state A).

	Distribution of wave energy			Sum
	(Primary wave)	(Primary wave)	(Resonant wave)	
	$a_{1,0}^2/\Pi$ (%)	$a_{0,1}^2/\Pi$ (%)	$a_{2,-1}^2/\Pi$ (%)	Π_0/Π (%)
Group B1	39.62	6.38	50.88	96.88
Group B2	38.52	39.08	17.30	94.90
Group B3	13.84	75.53	9.91	99.28

TABLE 17. Wave energy distribution of steady-state fully resonant waves when $\alpha_1 = 0$, $\alpha_2 = \pi/60$, $\epsilon = 1.0003$, $k_2 d = 3\pi/5$ and $k_2/k_1 = 1.06268$ (resonance state B).

5.1. *Steady-state fully resonant waves for* $\alpha_2 = \pi/60$

Substituting

$$\alpha_1 = 0, \quad \alpha_2 = \frac{\pi}{60}, \quad k_2 d = \frac{3\pi}{5} \tag{5.2}$$

into the nonlinear algebraic equation (4.2) gives three steady-state resonance states $k_2/k_1 = 0.946172, 1.06268, 2.205672$, corresponding to resonance states A, B and C, as in figure 1. Similarly, it is found that, for $k_2/k_1 = 0.946172$ (resonance state A) and $k_2/k_1 = 1.06268$ (resonance state B), there exist three steady-state fully resonant waves and, moreover, the resonant wave component can contain only a small proportion of the wave energy, as shown in tables 16 and 17. However, when $k_2/k_1 = 2.205672$ (corresponding to resonance state C), no steady-state fully resonant waves can be found. All these results further confirm the generalization of our conclusions in § 4.

5.2. *Resonant waves for* $\alpha_2 = 2\pi/45$

In this case, there also exist three steady-state resonance states, corresponding to $k_2/k_1 = 0.869372$ (resonance state A), 1.20261 (resonance state B) and 2.090427 (resonance state C), respectively. Similarly, in resonance states A and B, it is found that there also exist three steady-state fully resonant waves and that the resonant wave component may contain only a small proportion of the wave energy, as shown in tables 18 and 19, respectively. In particular, in resonance state B, the resonant wave component never contains the highest proportion of the wave energy, as shown in table 19, that is, the amplitude of the resonant wave component is always less than that of one of the primary ones: this is an extreme example to verify our conclusion that there exist multiple steady-state fully resonant waves in some cases, and that the resonant wave component may contain only a small proportion of the wave energy. However, no steady-state fully resonant waves are found for resonance state C. This once again confirms the generalization of our conclusions in § 4.

	Distribution of wave energy			Sum
	(Primary wave)	(Primary wave)	(Resonant wave)	
	$a_{1,0}^2/\Pi$ (%)	$a_{0,1}^2/\Pi$ (%)	$a_{2,-1}^2/\Pi$ (%)	Π_0/Π (%)
Group A1	9.01	11.65	79.30	99.96
Group A2	41.41	18.94	39.45	99.80
Group A3	41.76	49.47	8.69	99.92

TABLE 18. Wave energy distribution of three steady-state fully resonant waves when $\alpha_1 = 0$, $\alpha_2 = 2\pi/45$, $\epsilon = 1.0003$, and $k_2 d = 3\pi/5$ and $k_2/k_1 = 0.869372$ (corresponding to resonance state A).

	Distribution of wave energy			Sum
	(Primary wave)	(Primary wave)	(Resonant wave)	
	$a_{1,0}^2/\Pi$ (%)	$a_{0,1}^2/\Pi$ (%)	$a_{2,-1}^2/\Pi$ (%)	Π_0/Π (%)
Group B1	56.15	10.11	33.71	99.97
Group B2	41.76	40.33	17.87	99.96
Group B3	3.80	84.61	11.57	99.98

TABLE 19. Wave energy distribution of three steady-state fully resonant waves when $\alpha_1 = 0$, $\alpha_2 = 2\pi/45$, $\epsilon = 1.0003$, $k_2 d = 3\pi/5$ and $k_2/k_1 = 1.20261$ (corresponding to resonance state B).

This verifies that our conclusions given in §§ 4.1 and 4.2 have general application. Thus, when Phillips' resonance criterion (3.32) in finite water depth is exactly satisfied, there may indeed exist, in some cases, multiple steady-state fully resonant waves which have no exchange of wave energy, so that the corresponding wave spectrum is independent of time. Moreover, the resonant wave component may contain only a small proportion of the wave energy in some cases. However, such steady-state fully resonant waves do not always exist: for example, no steady-state fully resonant waves are found for resonance state C investigated in this article.

Physically speaking, such steady-state fully resonant progressive waves do exist in some cases, corresponding to a time-independent energy spectrum. However, even in these cases, there usually exist time-dependent periodic exchanges of wave energy governed by Jacobian elliptic functions, around the time-independent energy spectrum of a steady-state fully resonant wave, since it is hard to be exactly in such a balanced state in practice. So, our conclusions reported in this article might deepen and enrich understanding of the excellent work of Phillips (1960) and Benney (1962) on wave resonance.

6. Conclusions and discussion

Phillips (1960) gave the wave resonance criterion in his pioneering work; it was then re-derived by Longuet-Higgins (1962) using perturbation methods with the assumption that the amplitudes of two primary waves are of the same order but amplitudes of other wave components are much smaller. Phillips (1960) pointed out that, when the resonance criterion is satisfied, the amplitude of the resonant wave component, if zero initially, grows linearly with time t. However, the time t mentioned in Phillips' above conclusion must be small, otherwise the resonant wave component would contain most of the wave energy and thus break.

Benney (1962) established the evolution equations of wave mode amplitudes, and demonstrated the well-known time-dependent periodic exchange of wave energy governed by Jacobian elliptic functions, when Phillips' resonance criterion is fully or nearly satisfied. Mathematically speaking, the evolution equations of Benney (1962) correspond to a nonlinear initial value problem. Physically speaking, the time-dependent periodic exchange of wave energy leads to a time-dependent periodic energy spectrum.

Liao (2011) first investigated the existence of steady-state fully resonant wave systems in deep water when Phillips' resonance criterion is exactly satisfied. Here, the steady-state wave system consists of two progressive primary waves and all other wave components are due to nonlinear interaction and, further, each wave component has time-independent wavenumber, frequency and amplitude. Mathematically speaking, this is a nonlinear boundary-value problem. By means of the homotopy analysis method (HAM), Liao (2011) found, for the first time, that multiple steady-state fully resonant waves do indeed exist in deep water in some cases and, moreover, that the resonant wave component may contain only a small proportion of the wave energy.

To check the generalization of Liao's above-mentioned conclusions for steady-state fully resonant waves in deep water, we further investigate the existence of such steady-state fully resonant wave systems in water of finite depth, consisting of two progressive primary waves and all other components due to nonlinear interaction. Using the HAM as an analytic tool for the corresponding nonlinear boundary-value problem, it is found that such steady-state fully resonant waves in water of finite depth also exist in some cases, which have no exchange of wave energy between different wave components and thus a time-independent spectrum of energy, and further that the resonant component may contain only a small proportion of the wave energy. The same conclusions are obtained in various water depths by means of different angles between the two primary waves. It should be emphasized that qualitatively identical conclusions are obtained by using the famous Zakharov equation, as shown in appendix B. All of these verify the generalization of our conclusions concerning steady-state fully resonant waves. Further, it is worth mentioning that Madsen & Fuhrman (2012) numerically solved the harmonic resonance of irregular waves in water of finite depth, combined with a third-order perturbation approximation. Their numerical results, based on a high-order Boussinesq-type formulation, show a bound resonant wave field having constant amplitude in space, consistent with the steady-state fully resonant waves reported in this paper, although they did not find multiple steady-state resonance waves.

As reported in this article, in some cases (for example, all of resonance state C investigated in this article) steady-state fully resonant waves do not exist, so there only exist time-dependent periodic exchanges of wave energy as reported by Benney (1962). However, in some cases, such as resonance states A and B considered in this article, steady-state fully resonant waves do indeed exist with time-independent energy spectra. But even in these cases there usually exist time-dependent periodic exchanges of wave energy around a time-independent energy spectrum of a corresponding steady-state fully resonant wave, since it is hard to be exactly in such a balanced state in practice. This view might deepen our understanding of wave resonance and enrich the excellent work of Phillips (1960) and Benney (1962).

Note that Phillips' resonance criterion can be derived in the context of perturbation theory by assuming that only amplitudes of two primary waves are of the same order but others are at higher order of a small physical parameter. However, using the HAM in this article, we do not need any such assumption: this is an advantage of the

HAM over the perturbation approach. Further, the HAM provides a convenient way to guarantee the convergence of approximations: this differentiates the HAM from all other analytic techniques. It should be emphasized that the linear governing equation and the bottom boundary conditions are automatically satisfied, and, moreover, the averaged residual squares of the two boundary conditions on the free surface generally decrease to the level of 10^{-15} and 10^{-17}, respectively. So, from a mathematical viewpoint, we are quite sure that the steady-state fully resonant waves obtained are solutions of the nonlinear boundary-value problem governed by (2.1)–(2.4). Note that all steady-state fully resonant waves are obtained by means of the same analytic approach with the same code. So, if a resonant wave component with maximum amplitude is acceptable, we have identical reasons to believe that the resonant wave component with the smallest amplitude is acceptable too.

Our computations confirm that the resonant wave component is indeed of the same order as the primary ones. This is consistent with experimental and numerical results. Note that, in the context of perturbation theory, only the two primary waves are assumed to be initially of the same order. This assumption of the perturbation approach is correct only in the case of non-resonance. Restricted by this assumption, perturbation results (usually at the third order of approximation) contain the so-called secular terms when Phillips' criterion is satisfied, so 'the perturbation theory breaks down due to singularities in the transfer functions', as recently pointed out by Madsen & Fuhrman (2012). Unlike the perturbation approach, the HAM is entirely independent of any small/large physical parameters: it does not need to make any assumptions about the amplitudes of wave components. Note that our analytic HAM-based approach successfully avoids the so-called 'secular terms' or 'singularities in the transfer functions' of perturbation methods, and provides the multiple solutions of steady-state fully resonant waves for the first time. This illustrates the validity and great potential of the HAM for complicated nonlinear problems.

Note that two progressive primary waves with small amplitudes are considered in this paper, mainly because Phillips' resonance criterion is given for waves with small wave amplitude. Obviously, it would be very interesting to investigate steady-state fully resonant wave systems consisting of two or more primary waves with large wave amplitudes and all components due to nonlinear interaction. Further, it would be valuable to investigate steady-state fully resonant waves between two layer flows, or in periodically variable water depth, or with surface tension, and so on. In addition, the stability of steady-state fully resonant waves should also be investigated in detail.

Acknowledgements

The authors are indebted to Professor C. C. Mei (MIT, USA) for his valuable suggestions and discussions. We thank the reviewers for their valuable comments and suggestions. We thank the National Natural Science Foundation (Approval No. 10572095) and State Key Lab of Ocean Engineering (Approval No. GKZD010053, GKZD010056) for financial support. This work is also partly supported by the Lloyd's Register Educational Trust through the joint centre involving Shanghai Jiao Tong University, University College London and Harbin Engineering University. The Lloyd's Register Educational Trust is an independent charity working to achieve advances in transportation, science, engineering and technology education, training and research worldwide for the benefit of all.

Appendix A. Definitions of $\varDelta_m^\phi$, $\varDelta_m^\eta$, S_m, $\bar{S}_m$ and χ_m in (3.25) and (3.26)

Definitions of $\varDelta_m^\phi$, $\varDelta_m^\eta$, S_m, and $\bar{S}_m$ in (3.25) and (3.26) are given by

$$\begin{aligned}\varDelta_{m-1}^{\phi} = {}& \sigma_1^2\bar{\phi}_{m-1}^{2,0} + 2\sigma_1\sigma_2\bar{\phi}_{m-1}^{1,1} + \sigma_2^2\bar{\phi}_{m-1}^{0,2} + g\bar{\phi}_{z,m-1}^{0,0}\\ & - 2\left(\sigma_1\varGamma_{m-1,1} + \sigma_2\varGamma_{m-1,2}\right) + \varLambda_{m-1},\end{aligned} \tag{A 1}$$

$$\varDelta_{m-1}^{\eta} = \eta_{m-1} - \frac{1}{g}\left[(\sigma_1\bar{\phi}_{m-1}^{1,0} + \sigma_2\bar{\phi}_{m-1}^{0,1}) - \varGamma_{m-1,0}\right], \tag{A 2}$$

$$\bar{S}_n = \sum_{m=1}^{n-1}\left(\omega_1^2\beta_{2,0}^{n-m,m} + 2\omega_1\omega_2\beta_{1,1}^{n-m,m} + \omega_2^2\beta_{0,2}^{n-m,m} + g\gamma_{0,0}^{n-m,m}\right), \tag{A 3}$$

$$S_n = \sum_{m=0}^{n-1}\left(\omega_1^2\beta_{2,0}^{n-m,m} + 2\omega_1\omega_2\beta_{1,1}^{n-m,m} + \omega_2^2\beta_{0,2}^{n-m,m} + g\gamma_{0,0}^{n-m,m}\right), \tag{A 4}$$

where

$$\begin{aligned}\varGamma_{m,0} = {}& \frac{k_1^2}{2}\sum_{n=0}^{m}\bar{\phi}_n^{1,0}\bar{\phi}_{m-n}^{1,0} + \boldsymbol{k}_1\cdot\boldsymbol{k}_2\sum_{n=0}^{m}\bar{\phi}_n^{1,0}\bar{\phi}_{m-n}^{0,1}\\ & + \frac{k_2^2}{2}\sum_{n=0}^{m}\bar{\phi}_n^{0,1}\bar{\phi}_{m-n}^{0,1} + \frac{1}{2}\sum_{n=0}^{m}\bar{\phi}_{z,n}^{0,0}\bar{\phi}_{z,m-n}^{0,0},\end{aligned} \tag{A 5a}$$

$$\begin{aligned}\varGamma_{m,1} = {}& \sum_{n=0}^{m}\left(k_1^2\bar{\phi}_n^{1,0}\bar{\phi}_{m-n}^{2,0} + k_2^2\bar{\phi}_n^{0,1}\bar{\phi}_{m-n}^{1,1} + \bar{\phi}_{z,n}^{0,0}\bar{\phi}_{z,m-n}^{1,0}\right)\\ & + \boldsymbol{k}_1\cdot\boldsymbol{k}_2\sum_{n=0}^{m}\left(\bar{\phi}_n^{1,0}\bar{\phi}_{m-n}^{1,1} + \bar{\phi}_n^{2,0}\bar{\phi}_{m-n}^{0,1}\right),\end{aligned} \tag{A 5b}$$

$$\begin{aligned}\varGamma_{m,2} = {}& \sum_{n=0}^{m}\left(k_1^2\bar{\phi}_n^{1,0}\bar{\phi}_{m-n}^{1,1} + k_2^2\bar{\phi}_n^{0,1}\bar{\phi}_{m-n}^{0,2} + \bar{\phi}_{z,n}^{0,0}\bar{\phi}_{z,m-n}^{0,1}\right)\\ & + \boldsymbol{k}_1\cdot\boldsymbol{k}_2\sum_{n=0}^{m}\left(\bar{\phi}_n^{1,0}\bar{\phi}_{m-n}^{0,2} + \bar{\phi}_n^{0,1}\bar{\phi}_{m-n}^{1,1}\right),\end{aligned} \tag{A 5c}$$

$$\begin{aligned}\varGamma_{m,3} = {}& \sum_{n=0}^{m}\left(k_1^2\bar{\phi}_n^{1,0}\bar{\phi}_{z,m-n}^{1,0} + k_2^2\bar{\phi}_n^{0,1}\bar{\phi}_{z,m-n}^{0,1} + \bar{\phi}_{z,n}^{0,0}\bar{\phi}_{zz,m-n}^{0,0}\right)\\ & + \boldsymbol{k}_1\cdot\boldsymbol{k}_2\sum_{n=0}^{m}\left(\bar{\phi}_n^{1,0}\bar{\phi}_{z,m-n}^{0,1} + \bar{\phi}_n^{0,1}\bar{\phi}_{z,m-n}^{1,0}\right),\end{aligned} \tag{A 5d}$$

$$\begin{aligned}\varLambda_m = {}& \sum_{n=0}^{m}\left(k_1^2\bar{\phi}_n^{1,0}\varGamma_{m-n,1} + k_2^2\bar{\phi}_n^{0,1}\varGamma_{m-n,2} + \bar{\phi}_{z,n}^{0,0}\varGamma_{m-n,3}\right)\\ & + \boldsymbol{k}_1\cdot\boldsymbol{k}_2\sum_{n=0}^{m}\left(\bar{\phi}_n^{1,0}\varGamma_{m-n,2} + \bar{\phi}_n^{0,1}\varGamma_{m-n,1}\right),\end{aligned} \tag{A 5e}$$

with the definitions

$$\mu_{1,n} = \eta_n, \quad n \geqslant 1, \tag{A 6}$$

$$\mu_{m,n} = \sum_{i=m-1}^{n-1} \mu_{m-1,i}\eta_{n-i}, \quad m \geqslant 2, n \geqslant m, \tag{A 7}$$

$$\psi_{i,j}^{n,m} = \frac{\partial^{i+j}}{\partial \xi_1^i \partial \xi_2^j}\left(\frac{1}{m!}\frac{\partial^m \phi_n}{\partial z^m}\bigg|_{z=0} \right), \tag{A 8}$$

$$\beta_{i,j}^{n,0} = \psi_{i,j}^{n,0}, \tag{A 9}$$

$$\beta_{i,j}^{n,m} = \sum_{s=1}^{m} \psi_{i,j}^{n,s}\mu_{s,m} \quad m \geqslant 1, \tag{A 10}$$

$$\gamma_{i,j}^{n,0} = \psi_{i,j}^{n,1}, \tag{A 11}$$

$$\gamma_{i,j}^{n,m} = \sum_{s=1}^{m} (s+1)\psi_{i,j}^{n,s+1}\mu_{s,m} \quad m \geqslant 1, \tag{A 12}$$

$$\delta_{i,j}^{n,0} = 2\psi_{i,j}^{n,2}, \tag{A 13}$$

$$\delta_{i,j}^{n,m} = \sum_{s=1}^{m} (s+1)(s+2)\psi_{i,j}^{n,s+2}\mu_{s,m} \quad m \geqslant 1, \tag{A 14}$$

$$\bar{\phi}_n^{i,j} = \sum_{m=0}^{n} \beta_{i,j}^{n-m,m}, \tag{A 15}$$

$$\bar{\phi}_{z,n}^{i,j} = \sum_{m=0}^{n} \gamma_{i,j}^{n-m,m}, \tag{A 16}$$

$$\bar{\phi}_{zz,n}^{i,j} = \sum_{m=0}^{n} \delta_{i,j}^{n-m,m}. \tag{A 17}$$

For details, refer to Liao (2011, 2012).

Appendix B. Steady-state fully resonating quartet given by Zakharov's equation

A linearly resonating quartet, with wavenumbers $\boldsymbol{k}_j$ and frequencies ω_j, where $\boldsymbol{k}_j$ and $\omega_j, j = 1, 2, 3, 4$, are related by the linear dispersion relation $\omega_j^2 = gk_j \tanh(k_j d)$, satisfies the equations

$$\boldsymbol{k}_1 + \boldsymbol{k}_2 = \boldsymbol{k}_3 + \boldsymbol{k}_4, \quad \omega_1 + \omega_2 = \omega_3 + \omega_4. \tag{B 1}$$

Due to weak nonlinear effects, the actual frequencies of the waves, σ_j, are slightly different from ω_j, and also depend on the wave amplitudes. These changes are sometimes called Stokes' corrections. A fully resonating quartet is defined here as one that satisfies (B 1), as well as

$$\sigma_1 + \sigma_2 = \sigma_3 + \sigma_4. \tag{B 2}$$

Here we use Zakharov's equation to show that the amplitudes of fully resonating quartets can indeed be time-independent in some cases.

Zakharov (1968) assumed that the wave field can be divided into free and bound components. For the special resonant quartet

$$2\boldsymbol{k}_1 - \boldsymbol{k}_2 = \boldsymbol{k}_3, \tag{B 3}$$

$$2\omega_1 - \omega_2 = \omega_3, \tag{B 4}$$

the free components

$$\tilde{B}(\boldsymbol{k}, t) = B_1(t)\delta(\boldsymbol{k} - \boldsymbol{k}_1) + B_2(t)\delta(\boldsymbol{k} - \boldsymbol{k}_2) + B_3(t)\delta(\boldsymbol{k} - \boldsymbol{k}_3) \tag{B 5}$$

are governed by a discrete form of the Zakharov equation,

$$\mathrm{i}\frac{\mathrm{d}B_1}{\mathrm{d}t} = (T_{1,1,1,1}\,|B_1|^2 + 2T_{1,2,1,2}\,|B_2|^2 + 2T_{1,3,1,3}\,|B_3|^2)B_1 + 2T_{1,1,2,3}B_1^*B_2B_3\mathrm{e}^{\mathrm{i}\Delta\omega t}, \tag{B 6}$$

$$\mathrm{i}\frac{\mathrm{d}B_2}{\mathrm{d}t} = (2T_{2,1,2,1}\,|B_1|^2 + T_{2,2,2,2}\,|B_2|^2 + 2T_{2,3,2,3}\,|B_3|^2)B_2 + T_{2,3,1,1}B_3^*B_1^2\mathrm{e}^{-\mathrm{i}\Delta\omega t}, \tag{B 7}$$

$$\mathrm{i}\frac{\mathrm{d}B_3}{\mathrm{d}t} = (2T_{3,1,3,1}\,|B_1|^2 + 2T_{3,2,3,2}\,|B_2|^2 + T_{3,3,3,3}\,|B_3|^2)B_3 + T_{3,2,1,1}B_2^*B_1^2\mathrm{e}^{-\mathrm{i}\Delta\omega t}, \tag{B 8}$$

derived by Stiassnie & Shemer (1984), where

$$\Delta\omega = 2\omega_1 - \omega_2 - \omega_3, \tag{B 9}$$

$\mathrm{i} = \sqrt{-1}$ is the imaginary unit and $T_{a,b,c,d}$ is the kernel given in chapter 14 in Mei, Stiassnie & Yue (2005). Here, we use the formulas of $T_{a,a,a,a}$ and $T_{a,b,a,b}$ derived by Stiassnie & Gramstad (2009). The authors would like to thank Dr Odin Gramstad for his correction of the misprint in (4.10) given by Stiassnie & Gramstad (2009) during the private discussion. The expression of $T^{(S)}_{a,a,a,a}$ which we actually use in this paper is $T^{(S)}_{a,a,a,a} = -g/(16\pi^2(gd - Cg_a^2))\{4k_a^2[1 + (Cg_a/k_a\omega_a)(k_a^2 - (\omega_a^4/g^2))] + (k_a^2 - (\omega_a^4/g^2))^2(gd/\omega_a^2)\}$.

Assume that steady-state fully resonant waves exist. We search for the corresponding solution of $B_j(t)$ in the form

$$B_j(t) = b_j\mathrm{e}^{-\mathrm{i}\varOmega_j t}, \quad j = 1, 2, 3, \tag{B 10}$$

where $\varOmega_j = \sigma_j - \omega_j$ is a real constant, and

$$b_j = |b_j|\mathrm{e}^{\mathrm{i}\arg b_j}, \quad j = 1, 2, 3, \tag{B 11}$$

where $\arg b_j$ denotes the argument of b_j.

Substituting (B 5) and (B 10) into the wave elevation

$$\eta = \frac{1}{2\pi}\int_{-\infty}^{\infty}\left(\frac{\omega(\boldsymbol{k})}{2g}\right)^{1/2}\{\tilde{B}(\boldsymbol{k}, t)\mathrm{e}^{\mathrm{i}[\boldsymbol{k}\cdot\boldsymbol{x} - \omega(\boldsymbol{k})t]} + *\}\,\mathrm{d}\boldsymbol{k} \tag{B 12}$$

gives the steady-state resonant wave elevation

$$\eta = \sum_{j=1}^{3} a_j\cos(\boldsymbol{k}_j\cdot\boldsymbol{x} - \sigma_j t + \arg b_j), \tag{B 13}$$

where

$$a_j = \left(\frac{\omega_j}{2g}\right)^{1/2}\frac{|b_j|}{\pi}, \quad j = 1, 2, 3, \tag{B 14}$$

are constants independent of time. Note that, for the fully resonating special quartet (B 4), we have

$$2\Omega_1 - \Omega_2 = \Omega_3, \tag{B 15}$$

and thus

$$\Omega_j = (\epsilon - 1)\omega_j, \quad j = 1, 2, 3; \text{ see (4.1)}. \tag{B 16}$$

Substituting (B 10) and (B 15) into (B 6)–(B 8), we have the set of nonlinear algebraic equations

$$\Omega_1 = T_{1,1,1,1}\,|b_1|^2 + 2T_{1,2,1,2}\,|b_2|^2 + 2T_{1,3,1,3}\,|b_3|^2 + 2T_{1,1,2,3}|b_2||b_3|\mathrm{e}^{-\mathrm{i}\beta}, \tag{B 17}$$

$$\Omega_2 = 2T_{2,1,2,1}\,|b_1|^2 + T_{2,2,2,2}\,|b_2|^2 + 2T_{2,3,2,3}\,|b_3|^2 + T_{2,3,1,1}\frac{|b_3|\,|b_1|^2}{|b_2|}\mathrm{e}^{\mathrm{i}\beta}, \tag{B 18}$$

$$\Omega_3 = 2T_{3,1,3,1}\,|b_1|^2 + 2T_{3,2,3,2}\,|b_2|^2 + T_{3,3,3,3}\,|b_3|^2 + T_{3,2,1,1}\frac{|b_2|\,|b_1|^2}{|b_3|}\mathrm{e}^{\mathrm{i}\beta}, \tag{B 19}$$

where $\beta = 2\arg b_1 - \arg b_2 - \arg b_3$. We must have $\mathrm{e}^{\mathrm{i}\beta} = \pm 1$ so that the value of $|b_j|$ can be real. Instead of solving the algebraic equations (B 17)–(B 19), we can solve

$$\Omega_1 = T_{1,1,1,1}x^2 + 2T_{1,2,1,2}y^2 + 2T_{1,3,1,3}z^2 + 2T_{1,1,2,3}yz, \tag{B 20}$$

$$\Omega_2 = 2T_{2,1,2,1}x^2 + T_{2,2,2,2}y^2 + 2T_{2,3,2,3}z^2 + T_{2,3,1,1}\frac{zx^2}{y}, \tag{B 21}$$

$$\Omega_3 = 2T_{3,1,3,1}x^2 + 2T_{3,2,3,2}y^2 + T_{3,3,3,3}z^2 + T_{3,2,1,1}\frac{yx^2}{z}, \tag{B 22}$$

where $x = \pm|b_1|, y = \pm|b_2|, z = \pm|b_3|$ must be real constants, with the restriction $yz < 0$ corresponding to the case of $\mathrm{e}^{\mathrm{i}\beta} = -1$ and $yz > 0$ to $\mathrm{e}^{\mathrm{i}\beta} = 1$, respectively. For (4.1) with $\epsilon = 1.0003$, $k_2/k_1 = 0.913835$ and $k_2 d = 3\pi/5$, corresponding to resonance state A in figure 1, the above nonlinear algebraic equations (B 20)–(B 22) have 12 real solutions of x, y, z. They can be divided into three groups, called groups ZA1, ZA2 and ZA3 as listed in table 20, and each group has the same values of $|x|, |y|, |z|$, corresponding to $|b_1|, |b_2|, |b_3|$ in (B 17)–(B 19). Thus, the corresponding wave elevation (B 13) is steady-state, i.e. each corresponding amplitude a_j is independent of time. This confirms that the steady-state solution expression (2.19) for the HAM-based approach does indeed hold in some cases. Note that any $B_j(t)$ in each group has a time-independent norm $|B_j(t)|$ and, moreover, $|B_3(t)|$ related to the resonant wave component b_3 may be the largest, the smallest and in the middle, as shown in figure 6. These results qualitatively agree well with those obtained by the HAM-based approach for the same case.

For (4.1) with $\epsilon = 1.0003$, $k_2 d = 3\pi/5$ and $k_2/k_1 = 1.11165$, corresponding to resonance state B in figure 1, the nonlinear algebraic equations (B 20)–(B 22) also have 12 real solutions. They can be divided into three groups, called groups ZB1, ZB2 and ZB3 as listed in table 21, respectively. Therefore, the corresponding fully resonant waves are also steady-state, i.e. a_j in (B 13) is independent of time so the solution expression (2.19) for the HAM-based approach holds in this case too. Similarly, any $B_j(t)$ in each group has the same time-independent norm $|B_j(t)|$. It is found that $|B_3(t)|$ in group ZB1 is the largest, but $|B_3(t)|$ in groups ZB2 and ZB3 are the smallest, as shown in figure 7. These results qualitatively agree well with those given by the HAM-based approach.

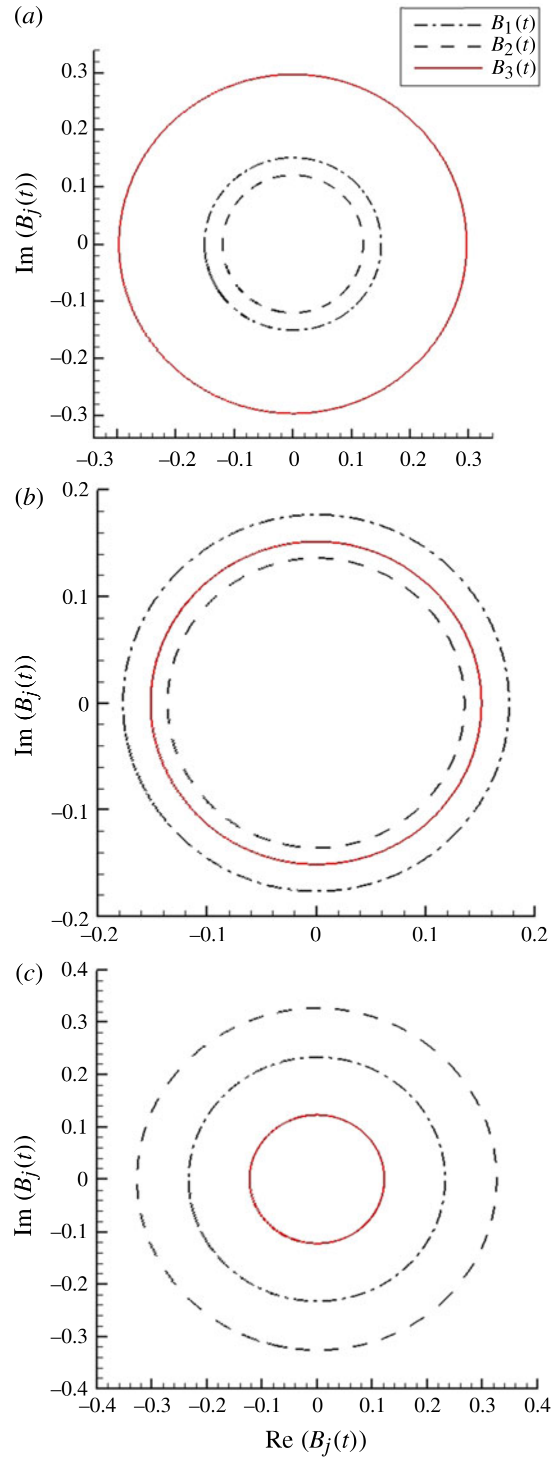

FIGURE 6. (Colour online) Time-independent norm $|B_j(t)|$ of (B 6)–(B 8) for (4.1) with $\epsilon = 1.0003$, $k_2 d = 3\pi/5$ and $k_2/k_1 = 0.913835$. (*a*) Group ZA1, (*b*) group ZA2, (*c*) group ZA3. Dash-dotted line, $B_1(t)$; dashed line, $B_2(t)$; solid line, $B_3(t)$.

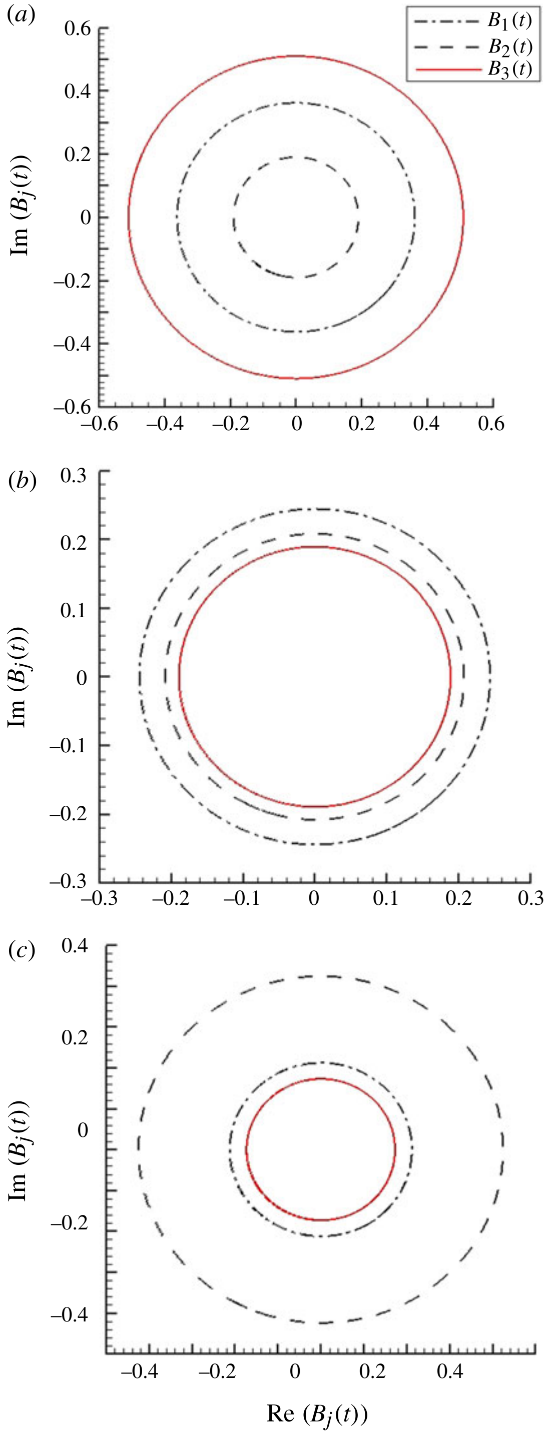

FIGURE 7. (Colour online) Time-independent norm $|B_j(t)|$ of (B 6)–(B 8) for (4.1) with $\epsilon = 1.0003$, $k_2 d = 3\pi/5$ and $k_2/k_1 = 1.11165$. (*a*) Group ZB1, (*b*) group ZB2, (*c*) group ZB3. Dash-dotted line, $B_1(t)$; dashed line, $B_2(t)$; solid line, $B_3(t)$.

Solution number	x	y	z
		Group ZA1	
1	−0.150906	−0.120227	0.29696
2	−0.150906	0.120227	−0.29696
3	0.150906	−0.120227	0.29696
4	0.150906	0.120227	−0.29696
		Group ZA2	
5	−0.176617	−0.135887	−0.151338
6	−0.176617	0.135887	0.151338
7	0.176617	−0.135887	−0.151338
8	0.176617	0.135887	0.151338
		Group ZA3	
9	−0.232949	−0.326529	0.122324
10	−0.232949	0.326529	−0.122324
11	0.232949	−0.326529	0.122324
12	0.232949	0.326529	−0.122324

TABLE 20. Real solutions of (B 20)–(B 22) for (4.1) with $\epsilon = 1.0003$, $k_2 d = 3\pi/5$ and $k_2/k_1 = 0.913835$, corresponding to resonance state A in figure 1. The values of x, y and z are obtained by means of $k_2 = \pi/5$ (m^{-1}) and $d = 3$ (m).

Solution number	x	y	z
		Group ZB1	
1	−0.361835	−0.190167	0.509642
2	−0.361835	0.190167	−0.509642
3	0.361835	−0.190167	0.509642
4	0.361835	0.190167	−0.509642
		Group ZB2	
5	−0.244212	−0.208006	−0.189132
6	−0.244212	0.208006	0.189132
7	0.244212	−0.208006	−0.189132
8	0.244212	0.208006	0.189132
		Group ZB3	
9	−0.212218	−0.424395	0.172923
10	−0.212218	0.424395	−0.172923
11	0.212218	−0.424395	0.172923
12	0.212218	0.424395	−0.172923

TABLE 21. Real solutions of (B 20)–(B 22) for (4.1) with $\epsilon = 1.0003$, $k_2 d = 3\pi/5$ and $k_2/k_1 = 1.11165$, corresponding to resonance state B in figure 1. The values of x, y and z are obtained by means of $k_2 = \pi/5$ (m^{-1}) and $d = 3$ (m).

For (4.1) with $\epsilon = 1.0003$ and $k_2 d = 3\pi/5$, there exist three steady-state fully resonant waves for both resonance states A and B. Further, the resonant wave component may contain only a small proportion of the wave energy, as shown in tables 22 and 23, where $\bar{\Pi}_0 = \sum_{i=1}^{3} a_i^2$. All these results qualitatively agree well with those given by the HAM-based approach described in §§ 4.1 and 4.2.

	Distribution of wave energy		
	Primary wave $a_1^2/\bar{\Pi}_0$ (%)	Primary wave $a_2^2/\bar{\Pi}_0$ (%)	Resonant wave $a_3^2/\bar{\Pi}_0$ (%)
Group ZA1	18.16	11.52	70.32
Group ZA2	42.99	25.45	31.56
Group ZA3	30.86	60.63	8.51

TABLE 22. Wave energy distribution of steady-state fully resonant waves for (4.1) with $\epsilon = 1.0003$, $k_2d = 3\pi/5$ and $k_2/k_1 = 0.913835$ (corresponding to resonance state A in figure 1), obtained by Zakharov's equation.

	Distribution of wave energy		
	Primary wave $a_1^2/\bar{\Pi}_0$ (%)	Primary wave $a_2^2/\bar{\Pi}_0$ (%)	Resonant wave $a_3^2/\bar{\Pi}_0$ (%)
Group ZB1	30.68	8.47	60.85
Group ZB2	43.01	31.20	25.79
Group ZB3	17.66	70.62	11.72

TABLE 23. Wave energy distribution of steady-state fully resonant waves for (4.1) with $\epsilon = 1.0003$, $k_2d = 3\pi/5$ and $k_2/k_1 = 1.11165$ (corresponding to resonance state B in figure 1), obtained by Zakharov's equation.

However, as listed in table 24, there exist no real solutions of (B 20)–(B 22) for (4.1) with $\epsilon = 1.0003$, $k_2d = 3\pi/5$ and $k_2/k_1 = 2.173797$, corresponding to resonance state C in figure 1. So, in this case, real values of $\pm|b_j|$ do not exist. In other words, all wave amplitudes are dependent on time, so a steady-state solution formula is impossible. Note that the steady-state solution expression (2.19) for the HAM-based approach does not hold in this case either. Therefore, using Zakharov's equation, we obtain qualitatively identical conclusions to those given by the HAM-based approach described in § 4.3.

Similarly, for (5.1) with $\alpha_2 = \pi/60$, Zakharov's equation admits three steady-state fully resonant waves when $k_2/k_1 = 0.946172$ and 1.06268, respectively, and the resonant wave component can contain only a small proportion of the wave energy, as shown in tables 25 and 26. However, no steady-state fully resonant waves are found when $k_2/k_1 = 2.205672$.

Similarly, for (5.1) with $\alpha_2 = 2\pi/45$, Zakharov's equation admits three steady-state fully resonant waves when $k_2/k_1 = 0.869372$ and 1.20261, respectively, and the resonant wave component can contain only a small proportion of the wave energy, as shown in tables 27 and 28. However, no steady-state fully resonant waves are found when $k_2/k_1 = 2.090427$.

In summary, using Zakharov's equation, it is found that multiple steady-state fully resonant waves exist in some cases and, moreover, the triad resonant wave component may indeed contain only a small proportion of the wave energy. All these results given by Zakharov's equation qualitatively agree well with those given by the HAM-based approach. This supports the validity and correctness of our conclusions based on the fully nonlinear wave equations and the HAM.

Finally, it should be mentioned that, quantitatively speaking, there are differences in the energy distribution between the results given by the fully nonlinear wave equation and Zakharov's equation. Such differences are probably due to the non-uniqueness of

Solution number	x	y	z
		Group ZC1	
1	−0.248103 − 0.723583i	−0.457127 + 0.232844i	0.23813 + 0.329231i
2	−0.248103 − 0.723583i	0.457127 − 0.232844i	−0.23813 − 0.329231i
3	−0.248103 + 0.723583i	−0.457127 − 0.232844i	0.23813 − 0.329231i
4	−0.248103 + 0.723583i	0.457127 + 0.232844i	−0.23813 + 0.329231i
5	0.248103 − 0.723583i	−0.457127 − 0.232844i	0.23813 − 0.329231i
6	0.248103 − 0.723583i	0.457127 + 0.232844i	−0.23813 + 0.329231i
7	0.248103 + 0.723583i	−0.457127 + 0.232844i	0.23813 + 0.329231i
8	0.248103 + 0.723583i	0.457127 − 0.232844i	−0.23813 − 0.329231i
		Group ZC2	
9	−0.0634453 − 0.756862i	−0.0483005 + 0.175302i	0.0940362 + 0.236329i
10	−0.0634453 − 0.756862i	0.0483005 − 0.175302i	−0.0940362 − 0.236329i
11	−0.0634453 + 0.756862i	−0.0483005 − 0.175302i	0.0940362 − 0.236329i
12	−0.0634453 + 0.756862i	0.0483005 + 0.175302i	−0.0940362 + 0.236329i
13	0.0634453 − 0.756862i	−0.0483005 − 0.175302i	0.0940362 − 0.236329i
14	0.0634453 − 0.756862i	0.0483005 + 0.175302i	−0.0940362 + 0.236329i
15	0.0634453 + 0.756862i	−0.0483005 + 0.175302i	0.0940362 + 0.236329i
16	0.0634453 + 0.756862i	0.0483005 − 0.175302i	−0.0940362 − 0.236329i

TABLE 24. Complex solutions of (B 20)–(B 22) for (4.1) with $\epsilon = 1.0003$, $k_2 d = 3\pi/5$ and $k_2/k_1 = 2.173797$, corresponding to resonance state C in figure 1. The values of x, y and z are obtained by means of $k_2 = \pi/5$ (m^{-1}) and $d = 3$ (m).

	Distribution of wave energy		
	Primary wave	Primary wave	Resonant wave
	$a_1^2/\bar{\Pi}_0$ (%)	$a_2^2/\bar{\Pi}_0$ (%)	$a_3^2/\bar{\Pi}_0$ (%)
Group ZA1	21.13	10.58	68.29
Group ZA2	42.91	26.80	30.29
Group ZA3	28.49	62.66	8.85

TABLE 25. Wave energy distribution of steady-state fully resonant waves for (5.1) with $\alpha_2 = \pi/60$ and $k_2/k_1 = 0.946172$ (corresponding to resonance state A), obtained by Zakharov's equation.

	Distribution of wave energy		
	Primary wave	Primary wave	Resonant wave
	$a_1^2/\bar{\Pi}_0$ (%)	$a_2^2/\bar{\Pi}_0$ (%)	$a_3^2/\bar{\Pi}_0$ (%)
Group ZB1	28.45	8.83	62.72
Group ZB2	42.91	30.15	26.94
Group ZB3	21.03	68.34	10.63

TABLE 26. Wave energy distribution of steady-state fully resonant waves for (5.1) with $\alpha_2 = \pi/60$ and $k_2/k_1 = 1.06268$ (corresponding to resonance state B), obtained by Zakharov's equation.

	Distribution of wave energy		
	Primary wave	Primary wave	Resonant wave
	$a_1^2/\bar{\Pi}_0$ (%)	$a_2^2/\bar{\Pi}_0$ (%)	$a_3^2/\bar{\Pi}_0$ (%)
Group ZA1	12.84	13.50	73.66
Group ZA2	43.12	23.09	33.79
Group ZA3	35.01	56.88	8.11

TABLE 27. Wave energy distribution of steady-state fully resonant waves for (5.1) with $\alpha_2 = 2\pi/45$ and $k_2/k_1 = 0.869372$ (corresponding to resonance state A), obtained by Zakharov's equation.

	Distribution of wave energy		
	Primary wave	Primary wave	Resonant wave
	$a_1^2/\bar{\Pi}_0$ (%)	$a_2^2/\bar{\Pi}_0$ (%)	$a_3^2/\bar{\Pi}_0$ (%)
Group ZB1	34.17	7.99	57.84
Group ZB2	43.15	33.17	23.68
Group ZB3	9.92	75.40	14.68

TABLE 28. Wave energy distribution of steady-state fully resonant waves for (5.1) with $\alpha_2 = 2\pi/45$ and $k_2/k_1 = 1.20261$ (corresponding to resonance state B), obtained by Zakharov's equation.

the finite-depth water-wave problem: see Whitham (1962) and Davey & Stewartson (1974). This non-uniqueness does not exist in infinitely deep water, for which the wave amplitudes calculated by the HAM-based approach (Liao 2011) are nearly the same as those calculated from Zakharov's equation, as shown in table 29.

	Amplitudes of wave elevation		
	Primary wave $\|a_1\|$	Primary wave $\|a_2\|$	Resonant wave $\|a_3\|$
Case Z1	0.0200286	0.0248057	0.0102774
Group I	0.0205119	0.0232118	0.0089752
Case Z2	0.0160173	0.0112368	0.0144903
Group II	0.0147561	0.0100249	0.0146433
Case Z3	0.0105689	0.0105201	0.0256609
Group III	0.0097124	0.0103225	0.0257646

TABLE 29. Amplitudes of steady-state fully resonant waves in deep water with $\alpha_2 = \pi/36$ and $k_2/k_1 = 0.8925$. Cases Z1, Z2 and Z3 are obtained by Zakharov's equation. Groups I, II and III are given by table 9 in Liao (2011).

REFERENCES

BENNEY, D. J. 1962 Non-linear gravity wave interactions. *J. Fluid Mech.* **14** (4), 577–584.

BRETHERTON, F. P. 1964 Resonant interactions between waves: the case of discrete oscillations. *J. Fluid Mech.* **20** (3), 457–479.

CHEN, Y. Y. 1990 Nonlinear interaction between two gravity wave trains in water of uniform depth. *J. Harbour Technol.* **5**, 1–46.

CRAIK, A. D. D. 1988 *Wave Interactions and Fluid Flows*. Cambridge University Press.

DAVEY, A. & STEWARTSON, K. 1974 On three-dimensional packets of surface waves. *Proc. R. Soc. Lond.* A **338** (1613), 101–110.

KATSARDI, V. & SWAN, C. 2011 The evolution of large non-breaking waves in intermediate and shallow water. Part 1. Numerical calculations of uni-directional seas. *Proc. R. Soc.* A **467** (2127), 778–805.

LIAO, S. J. 1992 Proposed homotopy analysis techniques for the solution of nonlinear problems. PhD thesis, Shanghai Jiao Tong University.

LIAO, S. J. 1999 A uniformly valid analytic solution of two-dimensional viscous flow over a semi-infinite flat plate. *J. Fluid Mech.* **385**, 101–128.

LIAO, S. J. 2003 *Beyond Perturbation: Introduction to the Homotopy Analysis Method*. CRC.

LIAO, S. J. 2010 An optimal homotopy-analysis approach for strongly nonlinear differential equations. *Commun. Nonlinear Sci. Numer. Simul.* **15** (8), 2003–2016.

LIAO, S. J. 2011 On the homotopy multiple-variable method and its applications in the interactions of nonlinear gravity waves. *Commun. Nonlinear Sci. Numer. Simul.* **16** (3), 1274–1303.

LIAO, S. J. 2012 *Homotopy Analysis Method in Nonlinear Differential Equations*. Springer & Higher Education Press.

LONGUET-HIGGINS, M. S. 1962 Resonant interactions between two trains of gravity waves. *J. Fluid Mech.* **12** (3), 321–332.

LONGUET-HIGGINS, M. S & SMITH, N. D. 1966 An experiment on third-order resonant wave interactions. *J. Fluid Mech.* **25** (3), 417–435.

MADSEN, P. A. & FUHRMAN, D. R. 2012 Third-order theory for multi-directional irregular waves. *J. Fluid Mech.* **698**, 304–334.

MCGOLDRICK, L. F., PHILLIPS, O. M., HUANG, N. E. & HODGSON, T. H. 1966 Measurements of third-order resonant wave interactions. *J. Fluid Mech.* **25** (3), 437–456.

MEI, C. C., STIASSNIE, M. & YUE, D. K. P. 2005 *Theory and Applications of Ocean Surface Waves: Nonlinear Aspects*, vol. 2. World Scientific.

ONORATO, M., OSBORNE, A. R., JANSSEN, P. A. E. M. & RESIO, D. 2009 Four-wave resonant interactions in the classical quadratic Boussinesq equations. *J. Fluid Mech.* **618**, 263–277.

PHILLIPS, O. M. 1960 On the dynamics of unsteady gravity waves of finite amplitude. Part 1. The elementary interactions. *J. Fluid Mech.* **9** (2), 193–217.

PHILLIPS, O. M. 1981 Wave interactions: the evolution of an idea. *J. Fluid Mech.* **106**, 215–227.

Stiassnie, M. & Gramstad, O. 2009 On Zakharov's kernel and the interaction of non-collinear wavetrains in finite water depth. *J. Fluid Mech.* **639** (1), 433–442.

Stiassnie, M. & Shemer, L. 1984 On modifications of the Zakharov equation for surface gravity waves. *J. Fluid Mech.* **143**, 47–67.

Whitham, G. B. 1962 Mass, momentum and energy flux in water waves. *J. Fluid Mech.* **12**, 135–147.

Zakharov, V. E. 1968 Stability of periodic waves of finite amplitude on the surface of a deep fluid. *J. Appl. Mech. Tech. Phys.* **9** (2), 190–194.